Supersymmetric scenarios with dominant radiative neutralino decay

Sandro Ambrosanio*
Randall Physics Laboratory, University of Michigan, Ann Arbor, Michigan 48109-1120

Barbara Mele†
INFN, Sezione di Roma 1 and University ''La Sapienza,'' Rome, Italy
(Received 5 September 1996)

The radiative decay of the next-to-lightest neutralino into a lightest neutralino and a photon is analyzed in the minimal supersymmetric standard model. We find that significant regions of the supersymmetric parameter space with large radiative branching ratios (up to about 100%) do exist. The radiative channel turns out to be enhanced when the neutralino tree-level decays are suppressed either ''kinematically'' or ''dynamically.'' In general, in the regions allowed by data from CERN LEP and not characterized by asymptotic values of the supersymmetric parameters, the radiative enhancement requires $\tan\beta \simeq 1$ and/or $M_1 \simeq M_2$, and negative values of μ. We present typical scenarios where these conditions are satisfied, relaxing the usual relation $M_1 = \frac{5}{3}\tan^2\theta_W M_2$, i.e., gaugino mass unification at the grand unified theory scale. The influence of varying the top-squark masses and mixing angle when the radiative decay is enhanced is also considered. Some phenomenological consequences of the above picture are discussed. [S0556-2821(97)01503-8]

PACS number(s): 14.80.Ly, 12.60.Jv

I. INTRODUCTION

Neutralinos ($\tilde{\chi}_i^0$, $i=1,...,4$; $m_{\tilde{\chi}_1^0} \leqslant \cdots \leqslant m_{\tilde{\chi}_4^0}$) are among the lightest supersymmetric (SUSY) partners predicted in the minimal supersymmetric standard model (MSSM) [1].[1] In particular, the $\tilde{\chi}_1^0$ is usually the lightest SUSY particle (LSP). Hence, for conserved R parity, $\tilde{\chi}_1^0$ is always present among the decay products of any superpartner, giving rise to large amounts of missing energy and momentum in the final states corresponding to pair production of SUSY particles in ee, $p\bar{p}$, or ep collisions. The heavier neutralinos have in general a rather complicated decay pattern towards the LSP, with possible intermediate steps involving other neutralinos and/or charginos as well as two-body decays with on-shell $Z^0/W^\pm$, Higgs bosons of sfermions in the final states [2]. Being the lightest visible neutralino, the next-to-lightest neutralino $\tilde{\chi}_2^0$ is of particular practical interest. It would be among the first SUSY partners to be produced at the CERN e^+e^- collider LEP 2 and at the Fermilab Tevatron [3,4].

The dominant $\tilde{\chi}_2^0$ decay channels are, in general, tree-level decays into a lightest neutralino and two standard fermions through either a (possibly on shell) Z^0 or sfermion exchange. Accordingly, the $\tilde{\chi}_2^0$ decays into a $\tilde{\chi}_1^0$ plus a l^+l^-, $\nu_l\bar{\nu}_l$, or $q\bar{q}$ pair. When $\tilde{\chi}_2^0$ is heavier than the lightest chargino, also cascade decays through a $\tilde{\chi}_1^\pm$ can become relevant. Hence, one can have, as final states, $l^+l'^-\nu_l\bar{\nu}_{l'}$, $l^\pm\nu_l q\bar{q}'$, $q_1\bar{q}_1'q_2\bar{q}_2'$, plus a $\tilde{\chi}_1^0$. An additional possibility is the two-body mode $\tilde{\chi}_2^0 \to \tilde{\chi}_1^0 h^0(A^0)$, when the Higgs boson(s) is (are) light enough [2,5]. This may give rise to events with a $bb/\tau^+\tau^-$ pair and missing energy and momentum ($\not{E}$ and $\not{p}$) in the detectors.

The radiative $\tilde{\chi}_2^0$ decay into a photon and a lightest neutralino $\tilde{\chi}_2^0 \to \tilde{\chi}_1^0\gamma$ provides a further decay channel with an even more interesting signature. Analytical formulas for the corresponding width can be found in Ref. [6].[2] Because of the higher-order coupling, this channel is characterized in general by rather low branching ratios (BR's). Nevertheless, a comprehensive study of the $\tilde{\chi}_2^0$ decay rates [5] shows that there are regions of the SUSY parameter space where the radiative decay is important and can even become the dominant $\tilde{\chi}_2^0$ decay.

In this paper, we perform a detailed phenomenological analysis of the decay $\tilde{\chi}_2^0 \to \tilde{\chi}_1^0\gamma$ in the MSSM. In particular, we analyze the regions of the SUSY parameter space where the radiative decay is enhanced. Some asymptotic regimes that give rise to large radiative BR's have been considered in Ref. [6]. In these particular cases, a considerable hierarchy is present among the different mass parameters of the MSSM Lagrangian, that by now corresponds to regions of the SUSY parameter space either partly or entirely excluded by LEP searches. In our study, we go beyond such asymptotic scenarios and consider regions of the SUSY parameter space where the parameters $M_{1,2}$ and $|\mu|$ have values roughly included in the range $[M_Z/4,\ 4M_Z]$. We relax the usual condition on the electroweak gaugino masses $M_1 = \frac{5}{3}\tan^2\theta_W M_2$, which holds [through one-loop renormalization group equa-

*Electronic address: ambros@umich.edu
†Electronic address: mele@roma1.infn.it

[1]In this paper, by MSSM we refer to the supersymmetric extension of the standard model with minimal gauge group and particle content. No additional assumptions (such as unification assumptions at a large scale) are understood, unless explicitly stated.

[2]In checking the results of Ref. [6], we found that the first line in Eq. (59), p. 281, should be more properly written as

$$G_L = 2\cos\theta_t[T_{3t}Z_i^{(-)} + e_t\tan\theta_W Z_{i1}] + \sin\theta_t Z_{i4}\frac{m_t}{m_W\sin\beta}.$$

In this way, it can also be correctly generalized to the $f=b,\tau,...$ case, by substituting T_{3t}, e_t, $\theta_t \to T_{3f}$, e_f, θ_f.

tions (RGE's)] when one assumes their unification at a scale $M_{\rm GUT}\approx 10^{16}$ GeV, where the gauge couplings assume the same value.[3] In this paper, we will treat $M_{1,2}$, as well as the masses of the individual sfermions, as low-energy, free parameters. As for the sfermion masses, we will assume for simplicity, some common value (or two different values for sleptons and squarks), whenever the individual mass values are not particularly relevant for the analysis.

As we will show, taking both M_1 and M_2 as free parameters can produce new interesting scenarios beyond the ones already considered in Ref. [5]. In that paper, we already singled out some regions of the parameter space where the tree-level $\widetilde{\chi}_2^0$ decays are suppressed and $B(\widetilde{\chi}_2^0\to\widetilde{\chi}_1^0\gamma)$ is large. There, we partly misinterpreted the origin of the suppression in a few points of the most promising regions in the (μ,M_2) plane, ascribing it to the particular physical composition of $\widetilde{\chi}_{1,2}^0$. It will be clear from the following more complete analysis that in those scenarios a *kinematical* suppression of the tree-level decays can be effective, in addition to a *dynamical* one. We indeed noticed in Ref. [5], that the two lightest neutralinos are nearly degenerate in the interesting cases and that their mass difference $(m_{\widetilde{\chi}_2^0}-m_{\widetilde{\chi}_1^0})$ grows monotonically with $\tan\beta$. Now, we will show how different mechanisms can contribute to the radiative BR enhancement. These scenarios will be thoroughly analyzed by a systematic investigation of the regions of the SUSY parameter space where a large $B(\widetilde{\chi}_2^0\to\widetilde{\chi}_1^0\gamma)$ regime may be present. For instance, a *dynamical* suppression of the $\widetilde{\chi}_2^0$ tree-level decays occurs when $\widetilde{\chi}_1^0$ and $\widetilde{\chi}_2^0$ have a different dominant physical composition in terms of gauginos and Higgsinos.

The latter scenario can have particular relevance for explaining events like the $e^+e^-\gamma\gamma+\not{E}_T$ event recently observed by the Collider Detector at Fermilab (CDF) Collaboration at the Tevatron [7]. That event, characterized by the presence of hard photons, electrons, and large missing transverse energy, can be hardly explained within the standard model (SM). A possible solution to this puzzle can be found within the minimal SUSY models, by interpreting the CDF event as a result of selectron- (or chargino-) pair production, provided a large BR for the neutralino decay into a LSP and a photon is predicted. More generally, the presence of a large radiative neutralino decay BR is crucial to obtain, within SUSY high rates for final states associated to a signature of the kind $\gamma\gamma+X+\not{E}$, where $X=l^+l^{(\prime)-}$, $q\overline{q}$,..., or *nothing*.

Two different SUSY ''models'' have been proposed up to now to explain the $e^+e^-\gamma\gamma+\not{E}_T$ CDF event [8,9,10].[4] The first one arises within theories with low-energy supersymmetry breaking, where the breaking is transmitted to the visible sector by nongravitational interactions [12]. In such a scenario, the gravitino $\widetilde{G}$ turns out to be naturally the LSP and, if light enough (i.e., for $m_{\widetilde{G}}\lesssim 1$ keV), it can couple to standard SUSY particles strongly enough to be of relevance for collider phenomenology [13]. If one assumes that the lightest *standard* SUSY particle is still the lightest neutralino and R parity is conserved, all the heavier SUSY particles produce, at the end of their decay chain, (at least) one $\widetilde{\chi}_1^0$. Then, $\widetilde{\chi}_1^0$ decays radiatively, $\widetilde{\chi}_1^0\to\widetilde{G}\gamma$, through its photino component, if the latter is not tuned to zero [14]. Assuming the $\widetilde{\chi}_1^0$ radiative decay occurs well into the detector (i.e., close enough to the main vertex, which requires $m_{\widetilde{G}}\lesssim 250$ eV), such a model can provide a satisfactory explanation of the $e^+e^-\gamma\gamma+\not{E}_T$ event [8,9]. Once low-scale SUSY breaking and very light gravitino scenarios are trusted, the presence of a large-BR $\widetilde{\chi}_1^0$ radiative decay and the consequent signature of hard and central photons and missing energy are almost automatic [8,9,14]. Although quite general, such a hypothesis does not allow to predict much about the SUSY parameters apart from $m_{\widetilde{G}}$. In particular, an interpretation of the CDF event within this framework can single out some ranges for the physical masses of the involved particles only on the basis of a careful analysis of the kinematical characteristics of the event [8,10]. No specific statements about the values of the parameters in the SUSY Lagrangian (M_1, M_2, μ, $\tan\beta$, etc.) and, hence, no detailed predictions of the general related collider phenomenology can be achieved.

Somehow opposite is the situation if the CDF event (or a general $\gamma\gamma+X+\not{E}$ event) is explained within the MSSM, where the gravitino is heavy, the lightest neutralino is the LSP and the hard photons and the missing energy are due to the one-loop $\widetilde{\chi}_2^0\to\widetilde{\chi}_1^0\gamma$ decay [8,10]. In this case, a certain adjustment of the MSSM parameters is required (both in the *dynamical*- and in the *kinematical*-enhancement scenarios) in order to get large radiative BR's and large rates for events with hard central photons and missing energy. Also, if the hard photons are emitted by rather soft $\widetilde{\chi}_2^0$'s, the *dynamical* enhancement is the most effective mechanism in this respect. Then, one is in general able to select rather narrow ranges of the SUSY parameters, if the $\gamma\gamma+X+\not{E}$ events are interpreted in this framework [8,10]. Hence, such a framework can be quite predictive also about the SUSY collider phenomenology that should show up in the future.

In this work, we intend to investigate the latter hypothesis in a general framework. We simply look for regions in the usual MSSM parameter space where the $\widetilde{\chi}_2^0\to\widetilde{\chi}_1^0\gamma$ decay has sizeable BR's. We find that in order to have a large $B(\widetilde{\chi}_2^0\to\widetilde{\chi}_1^0\gamma)$ (up to about 100%) one needs in general $\tan\beta\simeq 1$ and/or $M_1\simeq M_2$, in addition to $\mu<0$.[5] This is a quite general requirement, while further conditions on the gaugino mass parameters M_1, M_2, the Higgsino mass $|\mu|$, and $\tan\beta$ can guarantee either a *dynamical* or a *kinematical* enhancement of $B(\widetilde{\chi}_2^0\to\widetilde{\chi}_1^0\gamma)$. These two possibilities will give rise to rather different spectra for the emitted photons.

The effects on $B(\widetilde{\chi}_2^0\to\widetilde{\chi}_1^0\gamma)$ of varying all the masses in the sfermion sector is also considered. In particular, the characteristics of the top squark sector are quite relevant for the radiative decay width [16,17,6]. In our previous studies [3,5],

[3]Note that this not necessarily corresponds to relaxing all the gaugino mass unification conditions. One can still imagine that M_2 and M_3, that is the parameters which correspond to non-Abelian gauge groups, unify in the usual way, while the unification relation between M_1 and M_2 may be different from the usual one and unknown.

[4]As we were completing this paper, three other papers appeared which discuss the CDF event in various contexts [11].

[5]In this paper, we follow the same convention as in Ref. [1] for the sign of μ. We also assume $M_{1,2}\geq 0$ and $\tan\beta\geq 1$. Note that large values of $\tan\beta(\gtrsim 60)$ are disfavored by a radiative electroweak symmetry breaking in the MSSM [15]

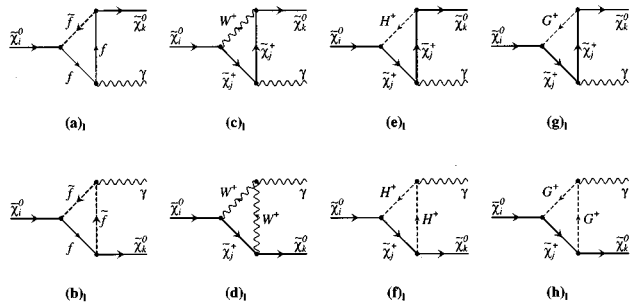

FIG. 1. Feynman diagrams for the radiative neutralino decay $\widetilde{\chi}_2^0 \to \widetilde{\chi}_1^0 \gamma$, in the gauge of Ref. [6]. For each graph shown, there is a further one with clockwise circulating particles in the loop.

we assumed all the left and right squarks degenerate in mass, in order to simplify the multiparameter dependence of the neutralino phenomenology. We also neglected the effects of a possible stop mixing. Here, we will examine the general case and we will see that the behavior of the $B(\widetilde{\chi}_2^0 \to \widetilde{\chi}_1^0 \gamma)$ can be affected by the top squark-sector parameters in different ways when the radiative BR is enhanced *dynamically* or *kinematically*.

The outline of the paper is the following. In Sec. II, we review the theory of the radiative neutralino decay in the MSSM and fix the notations. We also introduce the possible scenarios where a large $B(\widetilde{\chi}_2^0 \to \widetilde{\chi}_1^0 \gamma)$ regime can arise. In Secs. III and IV, respectively, we go through the SUSY parameter regions where a *dynamical* and a *kinematical* enhancement of the radiative decay can take place. In Sec. V, we perform a numerical analysis of the radiative BR in the relevant parameter regions. Finally, in Sec. VI, we study the top squark sector influence on the radiative neutralino decay. In Sec. VII, we draw our conclusions.

II. ENHANCED $B(\widetilde{\chi}_2^0 \to \widetilde{\chi}_1^0 \gamma)$ REGIMES

The radiative neutralino decay receives contributions, in a convenient gauge [6], from 16 graphs with all the charged (both SUSY and non-SUSY) standard particles flowing in the loop. The corresponding Feynman diagrams are displayed in Fig. 1. As a result, $\widetilde{\chi}_2^0 \to \widetilde{\chi}_1^0 \gamma$ is a very interesting process in itself, since it is influenced, to some extent, by all the parameters and sectors of the MSSM. However, being of higher order with respect to the main tree-level decays, the channel $\widetilde{\chi}_2^0 \to \widetilde{\chi}_1^0 \gamma$ typically has a BR not larger than a few percent. In previous studies [16], the possibility that $B(\widetilde{\chi}_2^0 \to \widetilde{\chi}_1^0 \gamma)$ gets large in the special case $\widetilde{\chi}_2^0 \simeq \widetilde{H}$, $\widetilde{\chi}_1^0 \simeq \widetilde{\gamma}$ has been considered, according to approximate formulae for the matrix element of the process, including only the main contributions from the $W^{\pm}/\widetilde{\chi}^{\pm}$ and $t/\widetilde{t}_1$ loops. In Ref. [6], after the full calculation of the matrix element and the decay width, two examples of scenarios with large $B(\widetilde{\chi}_2^0 \to \widetilde{\chi}_1^0 \gamma)$ are given, in two different limits. *Asymptotic* values of the relevant SUSY parameters, according to which the actual radiative processes are $\widetilde{\gamma} \to \widetilde{H} \gamma$ and $\widetilde{H}_1 \to \widetilde{H}_2 \gamma$, are considered (see below). In Ref. [5], by using the full calculation and assuming the gaugino-mass unification, we stress the presence of *nonasymptotic* regions of the parameter space, where the radiative process is still enhanced. In the following more general approach, we show that all the above scenarios are just particular realizations of the two main enhancement mechanisms for the radiative decay BR.

The naive expectation that the BR for $\widetilde{\chi}_2^0 \to \widetilde{\chi}_1^0 \gamma$ is negligible with respect to the BR's for the tree-level neutralino decays is not realized whenever the latter channels are suppressed for reasons that either do not affect or affect to a minor extent the radiative process. This can happen basically in two cases.

A. Dynamical suppression

Neutralinos are in general superpositions of gauginos ($\widetilde{\gamma}$ and $\widetilde{Z}$) and Higgsinos ($\widetilde{H}_a$ and $\widetilde{H}_b$).[6] The couplings of sfermions to neutralinos involve only the gaugino components [apart from terms $O(m_f/M_W)$, where m_f is the mass of the standard fermion also entering the vertex], while the Z^0 only couples through Higgsinos [1,17]. Then, the direct tree-level decays $\widetilde{\chi}_2^0 \to \widetilde{\chi}_1^0 f f$ require either simultaneous gaugino components in both $\widetilde{\chi}_1^0$ and $\widetilde{\chi}_2^0$ (for the sfermion-exchange process) or simultaneous Higgsino components (for the Z^0-exchange process). This is partly true even when the exchanged particles are on their mass shell, that is when the two-body channels $\widetilde{\chi}_2^0 \to f \widetilde{f}$ and/or $\widetilde{\chi}_2^0 \to Z^0 \widetilde{\chi}_1^0$ are open. The above requirement does not hold for the radiative decay, since in general both the gaugino and Higgsino components of neutralinos are involved in each graph of Fig. 1, apart from the diagrams (a) and (b) for a massless fermion f. Hence, whenever $\widetilde{\chi}_1^0(\widetilde{\chi}_2^0)$ is mainly a gaugino while $\widetilde{\chi}_2^0(\widetilde{\chi}_1^0)$ is dominated by the Higgsino components, the tree-level $\widetilde{\chi}_2^0$ width for direct decays falls down and the $B(\widetilde{\chi}_2^0 \to \widetilde{\chi}_1^0 \gamma)$ is enhanced. For pure gaugino and Higgsino states, $B(\widetilde{\chi}_2^0 \to \widetilde{\chi}_1^0 \gamma)$ can reach 100%. In particular regions of the parameter space, this picture can be modified by the presence of a light chargino. Indeed, the cascade decays $\widetilde{\chi}_2^0 \to \widetilde{\chi}_1^{\pm}(\to \widetilde{\chi}_1^0 f_1 \overline{f_1'}) f_2 \overline{f_2'}$, when kinematically allowed, can take place even for different physical composition of the two neutralinos, through $W^{\pm}$-exchange graphs involving both $\widetilde{W}_3$'s and $\widetilde{H}$'s. Note that a different dynamical suppression (that we call reduced dynamical suppression) of the tree-level direct decays can take place when the sfermions are heavy and the Z^0-exchange channel is dynamically suppressed by the presence of a dominant gaugino component in at least one of the two neutralinos. The latter case will be of some relevance in our following numerical analysis.

As for the decays into Higgs bosons, when $m_{h^0}(m_{A^0}) < (m_{\widetilde{\chi}_2^0} - m_{\widetilde{\chi}_1^0})$, the two-body channels $\widetilde{\chi}_2^0 \to \widetilde{\chi}_i^0 h^0(A^0)$, open up too. Naively, the latter do not seem to suffer from any dynamical suppression, since the MSSM predicts the vertex $\widetilde{Z}\widetilde{H}_i h^0(A^0)$. However, we will see that an effective dynamical suppression can be achieved when one of the two lightest neutralinos is dominated by a $\widetilde{\gamma}$ component (not just any gaugino). In this case, due to the absence of the $\widetilde{\gamma}\widetilde{H}_i h^0(A^0)$ vertex, the neutralino decays into Higgs bosons are depleted as well, and the $B(\widetilde{\chi}_2^0 \to \widetilde{\chi}_1^0 \gamma)$ can still be non-negligible.

[6]For the neutralino or chargino sectors, we use notations similar to Refs. [17, 18]. In particular, for the neutralino mixing matrix, we use the basis $(\widetilde{\gamma}, \widetilde{Z}, \widetilde{H}_a, \widetilde{H}_b)$, instead of $(\widetilde{B}, \widetilde{W}_3, \widetilde{H}_1, \widetilde{H}_2)$, used in Ref. [1]. This choice is particularly suitable for our purposes.

B. Kinematical suppression

When $\widetilde{\chi}_2^0$ and $\widetilde{\chi}_1^0$ tend to be degenerate in mass, the widths for the different $\widetilde{\chi}_2^0$ decay channels approach zero differently as the quantity $\epsilon=(1-m_{\widetilde{\chi}_1^0}/m_{\widetilde{\chi}_2^0})$ vanishes. For the radiative decay, one has [6]

$$\Gamma(\widetilde{\chi}_2^0\to\widetilde{\chi}_1^0\gamma)=\frac{g^2_{\widetilde{\chi}_1^0\widetilde{\chi}_2^0\gamma}}{8\pi}\frac{(m^2_{\widetilde{\chi}_2^0}-m^2_{\widetilde{\chi}_1^0})^3}{m^5_{\widetilde{\chi}_2^0}}\underset{\epsilon\to 0}{\sim}\frac{g^2_{\widetilde{\chi}_1^0\widetilde{\chi}_2^0\gamma}}{\pi}m_{\widetilde{\chi}_2^0}\epsilon^3, \tag{1}$$

where $g_{\widetilde{\chi}_1^0\widetilde{\chi}_2^0\gamma}\propto eg^2/16\pi^2$ is an effective coupling arising from the one-loop diagrams in Fig. 1 (in general a complicate function of all the masses and couplings to neutralinos of the particles circulating in the loops).

On the other hand, the three-body direct tree-level decays receive contributions from either Z^0-exchange graphs or sfermion-exchange graphs. The former, involving the Higgsino components only, in the same limit, lead to [6,17]

$$\Gamma(\widetilde{\chi}_2^0\to\widetilde{\chi}_1^0f\overline{f})_{Z^0\ \mathrm{exch}}\underset{\epsilon\to 0}{\sim}\frac{g^4f_wf_{\widetilde{H}}}{\pi^3}\frac{m^5_{\widetilde{\chi}_2^0}}{M_Z^4}\epsilon^5, \tag{2}$$

where $f_w\sim 10^{-2}$ and $f_{\widetilde{H}}$ is a number $\leqslant 1$, depending on the Higgsino content of the neutralinos (for pure Higgsinos, $f_{\widetilde{H}}=1$). Equation (2) implies a sum over five (six) flavors of final-state quarks (leptons). Finally, for the sfermion exchange, one has

$$\Gamma(\widetilde{\chi}_2^0\to\widetilde{\chi}_1^0f\overline{f})_{\widetilde{f}\ \mathrm{exch}}\underset{\epsilon\to 0}{\sim}\frac{g^4f'_wf_{\widetilde{\gamma}\widetilde{Z}}}{\pi^3}\frac{m^5_{\widetilde{\chi}_2^0}}{m^4_{\widetilde{f}}}\epsilon, \tag{3}$$

where $f'_w\sim 10^{-2}$ and $f_{\widetilde{\gamma}\widetilde{Z}}$ is a number $\leqslant 1$, depending on the photino and Z-ino content of the neutralinos.

As for the interference term of the Z^0 and sfermion exchange graph, we expect an intermediate behavior between Eqs. (2) and (3). This implies that, whenever in the direct decay the sfermion exchange is suppressed with respect to the Z^0 exchange (either because of large Higgsino components in $\widetilde{\chi}_{1,2}^0$ or because of rather heavy sfermions) the ratio of the direct tree-level- and the radiative-decay widths tends to vanish as ϵ^2, when $\epsilon\to 0$ ($m_{\widetilde{\chi}_2^0}\to m_{\widetilde{\chi}_1^0}$). Hence, e.g., for $(m_{\widetilde{\chi}_2^0}-m_{\widetilde{\chi}_1^0})\sim 10$ GeV, and $m_{\widetilde{\chi}_{1,2}^0}\approx M_Z$, the radiative decay BR will receive a factor of enhancement $\sim 10^2$ from kinematics. Also, the standard fermions in the final state of $\widetilde{\chi}_2^0\to\widetilde{\chi}_1^0ff$ can have a non-negligible mass when neutralinos are degenerate within a few GeV (e.g., when $f=\tau,b$). The latter may be an additional factor of depletion for the tree-level decays.

Regarding the cascade decays through light charginos, they are, in the same limit of negligible sfermion-exchange contributions, at least as kinematically suppressed as the normal direct three-body decays (indeed, $m_{\widetilde{\chi}_2^0}>m_{\widetilde{\chi}_1^\pm}>m_{\widetilde{\chi}_1^0}$ and the $W^\pm$-exchange graph behaves like the Z^0 exchange). On the other hand, in general, this class of decays will not be suppressed by a small coupling of the kind $f_wf_{\widetilde{H}}$ in Eq. (2). Furthermore, the two-body decay into Higgs bosons cannot take place when the mass difference between the two lightest neutralinos is less than a few tenths of GeV, because of the current experimental limits on $m(h^0)$ and $m(A^0)$ [19].

The conditions (a) and (b) can be translated into requirements on the SUSY parameters $\tan\beta$, μ, M_1, and M_2, which set the mass matrix of the neutralino sector. The tree-level neutralino mass matrix reads, in the convenient basis $[-i\widetilde{\gamma}, -i\widetilde{Z}, \widetilde{H}_a=\widetilde{H}_1\cos\beta-\widetilde{H}_2\sin\beta, \widetilde{H}_b=\widetilde{H}_1\sin\beta+\widetilde{H}_2\cos\beta]$:

$$\mathcal{M}_{\widetilde{\chi}^0}=\begin{bmatrix} M_1\cos^2\theta_W+M_2\sin^2\theta_W & (M_2-M_1)\sin\theta_W\cos\theta_W & 0 & 0\\ (M_2-M_1)\sin\theta_W\cos\theta_W & M_1\sin^2\theta_W+M_2\cos^2\theta_W & M_Z & 0\\ 0 & M_Z & \mu\sin 2\beta & -\mu\cos 2\beta\\ 0 & 0 & -\mu\cos 2\beta & -\mu\sin 2\beta \end{bmatrix}. \tag{4}$$

It is easy to recognize in Eq. (4) two 2×2 blocks, which correspond to (i) the gaugino mass terms, parametrized by M_1 and M_2 and mixed by the weak angle (their source is soft SUSY breaking), and (ii) the Higgsino mass terms, parametrized by μ and $\tan\beta=v_2/v_1$, whose source is a SUSY term in the MSSM Lagrangian, which mixes the Higgs doublets. Then, there are only two off-diagonal entries non included in the two 2×2 blocks, corresponding to $\widetilde{H}_a$-$\widetilde{Z}$ mixing terms and equal to M_Z, which come from the $H\widetilde{H}\widetilde{Z}$ couplings and the SUSY Higgs mechanism. As a consequence, apart from the asymptotic cases where $M_{1,2}$ and/or $|\mu|$ are much larger than the Z^0 mass, it is not possible to have either a pure $\widetilde{Z}$ or a pure $\widetilde{H}_a$. Hence, whenever a neutralino has a sizeable $\widetilde{Z}$ component, it must have a sizeable $\widetilde{H}_a$ component as well (and vice versa). This means that a neutralino can be a pure gaugino only when it is a photino, and a pure Higgsino can only be of the $\widetilde{H}_b$-type (sometimes called ''symmetric Higgsino'', with notation $\widetilde{H}_S$). Note also that when $M_1=M_2$ (or $\tan\beta=1$) the off-diagonal terms within the 2×2 gaugino (or Higgsino) block disappear. The limits $(M_1-M_2)\to 0$ and $\tan\beta\to 1$ will be crucial for the enhancement of the neutralino radiative decay.

The outcome of the neutralino mass matrix (4) in terms of the neutralino physical compositions and mass eigenstates has been extensively studied in Ref. [18]. We use the results of that analysis and concentrate here on what is relevant in order to realize either a dynamical or a kinematical enhancement of the $\widetilde{\chi}_2^0\to\widetilde{\chi}_1^0\gamma$ decay.

As already mentioned, some *asymptotic* regimes, where $\widetilde{\chi}_2^0\to\widetilde{\chi}_1^0\gamma$ is enhanced, were anticipated in Ref. [6]. Some enhancement is expected in the following two cases.

(i) Light-Neutralino Radiative Decay (M_1, M_2, $|\mu|\ll M_Z$). Then, a dynamical $\widetilde{\chi}_2^0\to\widetilde{\chi}_1^0\gamma$ enhancement is re-

alized, since $\widetilde{\chi}_1^0 \to \widetilde{\gamma}$ and $\widetilde{\chi}_2^0 \to \widetilde{H}_b$ or vice versa. In Ref. [6], the limit $\mu=0$, $\widetilde{\gamma} \to \widetilde{H}\gamma$ is treated analytically. Such small values of the parameters are not yet excluded by LEP data, provided $1 \leqslant \tan\beta \leqslant 2$ (what is called sometimes ''light Higgsino-gaugino window'' [20]). In fact, in this particular region, a number of things happens: (a) when $|\mu|/M_Z$, $M_2/M_Z \to 0$, the chargino mass generally satisfies the current LEP lower bounds; (b) if also $M_1/M_Z \to 0$, the neutralino mass eigenstates are $\widetilde{\gamma}, \widetilde{H}_b$ (with mass eigenvalue $\to 0$) and the symmetric and antisymmetric combinations of $\widetilde{Z}$ and $\widetilde{H}_a$ (with mass $\to M_Z$). Then, when $\tan\beta \to 1$, the light $\widetilde{H}_b$ decouples and the neutralinos can only interact with the Z^0 boson through the vertex $Z^0 \widetilde{H}_a \widetilde{H}_b$, which is largely suppressed by the phase space at LEP1 energies, since $[m(\widetilde{H}_a) + m(\widetilde{H}_b)] \simeq M_Z$. As a result, the data on the Z^0 peak can hardly constrain this particular region. For instance, in Ref. [21], the analysis is performed by considering the bounds on $\Gamma(Z^0 \to \widetilde{\chi}_1^0 \widetilde{\chi}_1^0)$ from the invisible Z^0 width and those on $\Gamma(Z^0 \to \widetilde{\chi}_1^0 \widetilde{\chi}_2^0, \widetilde{\chi}_2^0 \widetilde{\chi}_2^0)$ from the direct search of neutralinos. However, only the decays $\widetilde{\chi}_2^0 \to \widetilde{\chi}_1^0 Z^{(*)} \to \widetilde{\chi}_1^0 f\bar{f}$ are fully taken into account, while the radiative decay, although generally dominant in this region, is not properly stressed. In the analysis of Ref. [20], a tighter BR bound from the radiative neutralino decay has been included as well as the effects of data taken at $\sqrt{s}$ above M_Z. In spite of that, part of the region in the (μ, M_2) plane with $M_2, |\mu| \lesssim 10$ GeV still survives for $\mu<0$ and $\tan\beta$ close to 1. This region is wider when M_1 is taken as a free parameter and allowed to be quite larger than M_2. Some significant improvements in probing the above region could come from a careful analysis of the data of the recent LEP short runs at $\sqrt{s}=130$ and 136 GeV and those of the near future at $\sqrt{s}=161$ and 172 GeV. If the light gaugino-Higgsino scenario is realized, all charginos and neutralinos are expected to have masses in the kinematical reach of LEP2 and should not escape detection.

(ii) Higgsino-to-Higgsino Radiative Decay ($|\mu|$, $M_Z \ll M_1$, $M_2 \approx$ TeV). This corresponds to a particular asymptotic case of the kinematical $\widetilde{\chi}_2^0 \to \widetilde{\chi}_1^0 \gamma$ enhancement. Indeed, in this situation the two lightest neutralinos have nearly degenerate masses close to $|\mu|$, and are both almost pure Higgsinos. Hence, the direct tree-level decays can only proceed through Z^0-exchange graphs and the ratio between the corresponding width and the $\widetilde{H}_{1,2} \to \widetilde{H}_{2,1}\gamma$ width can be obtained from Eqs. (2) and (1), and is independent of the sfermion masses. In a sense, this is an optimization of the *kinematical*-suppression mechanism, since the presence of contributions from the sfermion-exchange diagrams tends to cancel this suppression [cf. Eq. (3)]. On the other hand, in the present case, the factor $f_{\widetilde{H}}$ in the numerator of Eq. (2) is close to its maximum 1, hence depleting the radiative-BR enhancement. In the asymptotic limit [6], one finds

$$\frac{\Gamma(\widetilde{H}_1 \to \widetilde{H}_2 \gamma)}{\Gamma(\widetilde{H}_1 \to \widetilde{H}_2 f\bar{f})} \sim 0.3 C^2 \alpha_{\rm em} \left[\frac{M_1 M_2}{\mu(M_1 + M_2 \tan^2\theta_W)} \right]^2, \qquad (5)$$

where C is a number of order unity weakly dependent on the ratio M_W^2/μ^2. Here, for large $M_{1,2}$, values of $|\mu| \lesssim M_Z/2$ are generally already excluded by LEP1–LEP1.5 data, since they lead to chargino masses lighter than 45–50 GeV. Hence, Eq. (5) tells us that one needs *very* large values of $M_{1,2}$ to get a significant enhancement of the radiative decay through this mechanism. In addition, in this region, $\widetilde{\chi}_2^0$ can often decay through cascade channels into a lighter chargino with a non-negligible branching fraction. Numerically, by using the full formulas, we checked that $B(\widetilde{\chi}_2^0 \to \widetilde{\chi}_1^0 \gamma) \lesssim 10\%$ always for $M_{1,2} \lesssim 2$–3 TeV, and $|\mu| \gtrsim 45$–50 GeV. Furthermore, it turns out that to have a sizeable radiative decay in this case (that is to suppress both direct and cascade tree-level decays), one always has to enforce the condition $(m_{\widetilde{\chi}_2^0} - m_{\widetilde{\chi}_1^0}) \lesssim 2-3$ GeV, which critically restricts the photon energy.

Note that, for nearly degenerate Higgsinos, the radiative corrections may actually spoil the enhancement mechanism or, at least, render the tree-level analysis rather inaccurate. For instance, the Higgsino-mass splittings in this region can receive radiative corrections as large as their tree-level values [i.e., up to $\pm(5$–$10)$ GeV], if the mixing between the two top squarks is large [22].

Now, we want to extend the quoted studies by analyzing the more general framework where either a dynamical or a kinematical $\widetilde{\chi}_2^0 \to \widetilde{\chi}_1^0 \gamma$ enhancement can be realized, without assuming any particular hierarchy between the SUSY parameters and relaxing the usual unification condition on the gaugino masses. We will not concentrate on particular limits of the SUSY parameters such as M_1 or $M_2 \to 0$ or $|\mu| \to 0$, since they have been either already excluded by LEP data or discussed above.

In the following, we will neglect the effects of the radiative corrections on the neutralino mass matrix elements. In Ref. [23], the full calculation has been carried out. Regarding the radiative corrections to the neutralino mass eigenvalues, they are found to be generally at the level of 3–8 % and of the same sign (positive) for all the mass eigenvalues. Only occasionally, the lightest neutralino mass can receive larger corrections. No conclusion can be easily extracted from that analysis about whether or not and how much the radiative corrections may change the composition of a neutralino eigenstate and, in particular, to what extent, for instance, an almost pure photino at the tree level, could turn out to be a more mixed state at the one-loop level. Our scenarios for an enhanced radiative-decay regime rely on a certain amount of adjustment between different SUSY parameters in order to get either pure compositions for the eigenvectors or degeneracy for the eigenvalues of the neutralino mass matrix. As for the kinematical-enhancement mechanism, we will show that a mass difference $(m_{\widetilde{\chi}_2^0} - m_{\widetilde{\chi}_1^0}) \sim 10$ GeV, with $m_{\widetilde{\chi}_{1,2}^0} \approx M_Z$, is in general sufficiently small to get a $B(\widetilde{\chi}_2^0 \to \widetilde{\chi}_1^0 \gamma)$ of order 40% or more. Since the higher-order corrections to the neutralino masses have generally a fixed sign, one can expect a common shift of the different masses, while the relative mass differences change only slightly. Thus, we expect that the kinematical suppression keeps almost unchanged for $(m_{\widetilde{\chi}_2^0} - m_{\widetilde{\chi}_1^0}) \sim 10$ GeV and that our treatment substantially holds even after radiative corrections, with a possible slight redefinition of the interesting regions in the SUSY parameter space. Concerning the dynamical-enhancement mechanism, similar arguments may be used, although in this case there are less clues to guess the effects of radiative corrections. However, we will see that the amount of parameter adjustment required for the mechanism to be effective is not very large. For instance, there are sig-

nificant regions in the parameter space where $|\langle\widetilde{\chi}^0_{1,2}|\widetilde{H}_b\rangle|^2$ and/or $|\langle\widetilde{\chi}^0_{2,1}|\widetilde{\gamma}\rangle|^2$ are *only* about 0.8 and the dynamical suppression is still effective, with the $B(\widetilde{\chi}^0_2\to\widetilde{\chi}^0_1\gamma)$ of order 50% or more. Hence, an adjustment of the parameters at the level of 20% should survive the inclusion of the radiative corrections.

An additional remark is due for the case of the kinematical enhancement mechanism. Since the latter arises from situations where the two lightest neutralinos are close in mass, a too strong degeneracy may prevent the experimental detection of the $\widetilde{\chi}^0_2$ decay, due to the emission of too soft photons. In general, one can ensure the presence of a useful experimental signature and the phenomenological relevance of the neutralino radiative decay by requiring $(m_{\widetilde{\chi}^0_2}-m_{\widetilde{\chi}^0_1})$ $\gtrsim$10 GeV. This, of course, effectively depletes the actual $B(\widetilde{\chi}^0_2\to\widetilde{\chi}^0_1\gamma)$ that can be achieved by the kinematical mechanism in a real experimental framework. On the other hand, if the available c.m. energy is large enough, the $\widetilde{\chi}^0_2$ can receive a sizeable boost, even when $(m_{\widetilde{\chi}^0_2}-m_{\widetilde{\chi}^0_1})$ is very small (for instance, when produced in association with a $\widetilde{\chi}^0_1$ at LEP2, or with a $\widetilde{\chi}^\pm_1$ at the Tevatron). In order to assess to what extent this is true, one can take into account that, assuming an isotropic radiative decay of the produced $\widetilde{\chi}^0_2$ (that is neglecting spin-correlation effects), the resulting photon has a flat energy distribution in the laboratory, with end points:

$$E(\gamma)_{\min,\max}=\left(\frac{E_2}{m_{\widetilde{\chi}^0_2}}\mp\sqrt{\frac{E_2^2}{m^2_{\widetilde{\chi}^0_2}}-1}\right)\left(\frac{m^2_{\widetilde{\chi}^0_2}-m^2_{\widetilde{\chi}^0_1}}{2m_{\widetilde{\chi}^0_2}}\right),$$

where E_2 is the production energy of the $\widetilde{\chi}^0_2$ in the laboratory.

III. DYNAMICAL $\widetilde{\chi}^0_2\to\widetilde{\chi}^0_1\gamma$ ENHANCEMENT

As already seen, requiring one pure gaugino and one pure Higgsino eigenstate from the matrix (4) implies both:

$$M_1=M_2 \tag{6}$$

and

$$\tan\beta=1. \tag{7}$$

One then has a pure $\widetilde{\gamma}$ with mass $M_1(=M_2)$ and a pure $\widetilde{H}_b$ of mass $(-\mu)$ in the neutralino spectrum. In this limit, the other two neutralinos are mixtures of $\widetilde{H}_a$ and $\widetilde{Z}$ with mass eigenvalues (including their sign)[7] [18]

$$m^{(\pm)}_{\widetilde{H}_a-\widetilde{Z}}=\frac{1}{2}\left[M_2+\mu\pm\sqrt{(M_2-\mu)^2+4M_Z^2}\right] \tag{8}$$

and mixing angle

$$\begin{Bmatrix}\sin\phi\\ \cos\phi\end{Bmatrix}=\frac{1}{\sqrt{2}}\left[1\pm\frac{M_2-\mu}{\sqrt{(M_2-\mu)^2+4M_Z^2}}\right]^{1/2} \tag{9}$$

Requiring that the pure states correspond to the lightest neutralinos, $\widetilde{\chi}^0_1$ and $\widetilde{\chi}^0_2$, the absolute values of both the eigenvalues in Eq. (8) have to be larger than both M_1 (or M_2) and $|\mu|$. In the parameter space not yet excluded by the LEP data, this can be achieved only if

$$\mu<0. \tag{10}$$

Indeed, when μ is positive, the smallest absolute value in Eq. (8) corresponds to choosing the negative sign before the square root. It is then sufficient to look at $m^{(-)}_{H-Z}$. The latter is always smaller (greater) than both μ and M_2, whenever μ and M_2 are larger (smaller) than $M_Z/2$. On the other hand, if $\mu<M_Z/2<M_2$ or $M_2<M_Z/2<\mu$, $m^{(-)}_{H-Z}$ can still (but not necessarily has to) be large enough to allow the mass ordering needed for the dynamical suppression. However, values of M_2 and/or $|\mu|\lesssim M_Z/2$, with μ positive, are generally excluded by LEP data. This is true either because of the chargino-mass bound, or because of the direct searches of neutralinos, even without gaugino-mass unification assumptions, and even in that window with very small $|\mu|$ and M_2 we treated above, for any $\tan\beta$. As a result, the dynamical enhancement can be present only for $\mu<0$. Note that the eigenvalue $m^{(-)}_{H-Z}$ corresponds to a massless neutralino when $\mu=M_2=M_Z$.

Quite different is the situation for $\mu<0$. Points in the SUSY parameter space where $m^{(\pm)}_{H-Z}$ are both heavier than $|\mu|$ and M_2 do exist for small values of $|\mu|$ and/or M_2. This is also true for large values of $|\mu|$ and M_2, i.e., far away from the LEP exclusion region. For instance, let's examine the case $\mu=-M_Z$. In this case, whenever $0\leqslant M_2<M_Z/2$, $|m^{(+)}_{H-Z}|$ is always less than $|\mu|$ and corresponds to the next-to-lightest neutralino, the lightest one being the photino with mass $M_1=M_2$. Then, no dynamical enhancement can take place. For $M_Z/2<M_2<M_Z(1+\sqrt{3})/2$, the neutralino eigenstates corresponding to $m^{(\pm)}_{H-Z}$ are always the two heaviest ones. Then, the radiative decay $\widetilde{H}_b\to\widetilde{\gamma}\gamma$, for $M_2<M_Z$, or $\widetilde{\gamma}\to\gamma\widetilde{H}_b$, for $M_2>M_Z$, benefits from a strong dynamical suppression of the tree-level decays. When M_2 gets larger than $1.37M_Z$, $m^{(-)}_{H-Z}$ becomes the next-to-lightest neutralino, while $\widetilde{H}_b$ is the lightest one. Once more, no dynamical enhancement can occur. This rather complex behavior generates sharp and well outlined contours for the $B(\widetilde{\chi}^0_2\to\widetilde{\chi}^0_1\gamma)$ in the (M_1,M_2) plane, in the vicinity of the diagonal $M_1=M_2$ (see Sec. V).

Of course, when (M_1-M_2) and $(\tan\beta-1)$ go away from 0, all the arguments given above, including the condition (10), have to be intended in a weaker sense. Large radiative BR's can be obtained, even in points of the parameter space where $|M_1-M_2|\lesssim M_Z/2$ and $\tan\beta\lesssim 2$. As for the validity of the condition (10) in a less restricted case, one has to note that a massless (or very light) state is present whenever the equation

$$M_1M_2\mu=(M_1\cos^2\theta_W+M_2\sin^2\theta_W)M_Z^2\sin2\beta \tag{11}$$

approximately holds [18]. This implies a positive μ. For general values of $M_{1,2}$ and $\tan\beta$, this state is a superposition of

[7]Of course, the physical neutralino masses are always positive, but the sign of the mass eigenvalue has its own physical meaning, being connected to the neutralino CP quantum numbers and entering the expressions, in the basis we adopt, of the Feynman amplitudes for processes involving neutralinos [1,17,18,24]

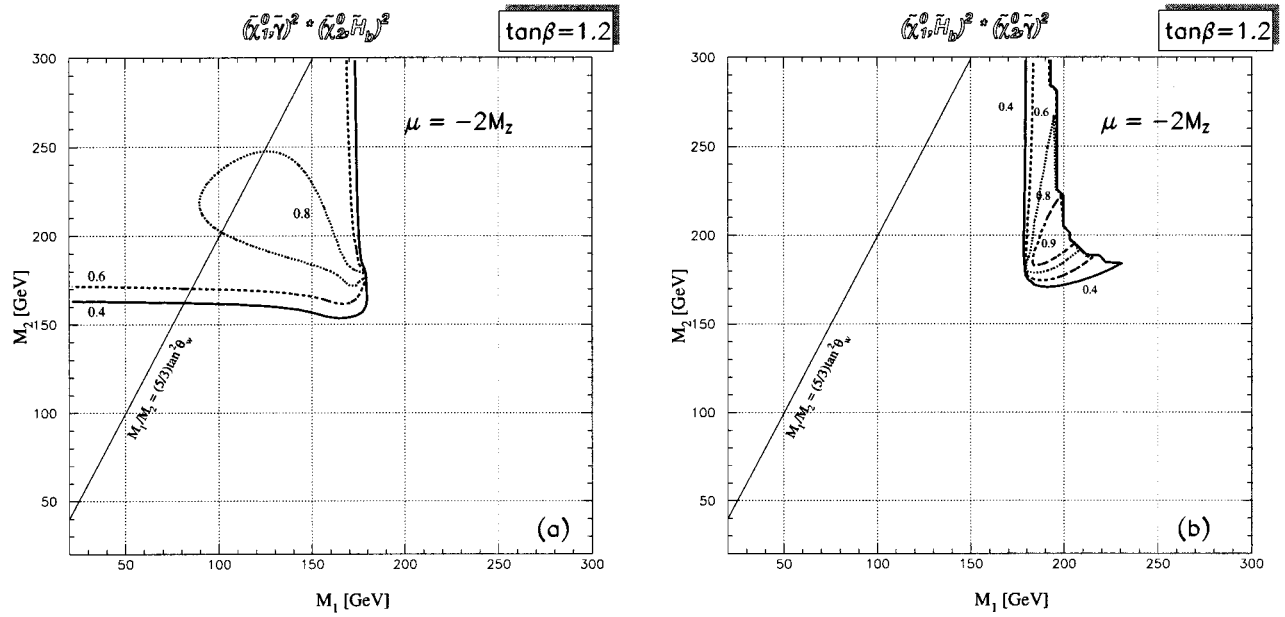

FIG. 2. Contour plot for the quantities: (a) $A=\langle\widetilde{\chi}_1^0|\widetilde{\gamma}\rangle^2\langle\widetilde{\chi}_2^0|\widetilde{H}_b\rangle^2$ and (b) $B=\langle\widetilde{\chi}_1^0|\widetilde{H}_b\rangle^2\langle\widetilde{\chi}_2^0|\widetilde{\gamma}\rangle^2$ ($A,B\leqslant 1$), in the case $\tan\beta=1.2$, $\mu=-2M_Z$. A and B give a hint of the ''purity'' of the limit $\widetilde{\chi}_1^0=\widetilde{\gamma}$, $\widetilde{\chi}_2^0=\widetilde{H}_B$ or vice versa. The line corresponding to gaugino-mass unification is also shown.

all the four interaction eigenstates. When $(M_1-M_2)\to 0$ its photino component tends to vanish, while its $\widetilde{H}_b$ component gets smaller and smaller as $\tan\beta\to 1$. Hence, in general, in a wide region in the vicinity of the curve defined by Eq. (11) in the plane (M_1,M_2), the lightest neutralino (or the next-to-lightest one) is a mixed state made of Higgsino–Z-ino and no dynamical-enhancement mechanism can be present, even if $M_1\simeq M_2$ and $\tan\beta\simeq 1$.

In our numerical analysis, we have not found any case of sizeable dynamical suppression for positive values of μ, in the allowed regions. Note that, for a positive μ, a very light chargino can be present. In particular, if

$$M_2\mu=M_W^2\sin 2\beta \tag{12}$$

the light chargino is massless. This gives rise to ''forbidden'' regions in the SUSY-parameter space in the positive-μ case, where our basic assumption LSP$=\widetilde{\chi}_1^0$ may not be satisfied.

On the other hand, even if $m_{\widetilde{\chi}_1^\pm}>m_{\widetilde{\chi}_1^0}$, the chargino often turns out to be lighter than the $\widetilde{\chi}_2^0$, opening the cascade channels, which do not suffer from dynamical suppression. This happens, for low $\tan\beta$, only rarely for $\mu<0$ and often for $\mu>0$, and provides a further explanation for the lack of significant $B(\widetilde{\chi}_2^0\to\widetilde{\chi}_1^0\gamma)$-enhancement regions in the positive-μ case.

In order to get a general insight of the neutralino physical composition pattern, we show in Figs. 2–4 the behavior in the (M_1,M_2) plane of the quantities $A=\langle\widetilde{\chi}_1^0|\widetilde{\gamma}\rangle^2\langle\widetilde{\chi}_2^0|\widetilde{H}_b\rangle^2$ and $B=\langle\widetilde{\chi}_1^0|\widetilde{H}_b\rangle^2\langle\widetilde{\chi}_2^0|\widetilde{\gamma}\rangle^2$ (A, $B<1$), which express the neutralino physical purity in the dynamical enhancement framework. We also study the effect of varying both the μ and $\tan\beta$ values in the interesting ranges. In the following, we will see that, in order to achieve an appreciable dynamical enhancement of $B(\widetilde{\chi}_2^0\to\widetilde{\chi}_1^0\gamma)$, either A or B should be as high as 0.8–0.9. This condition is fulfilled in a substantial portion of the (M_1,M_2) plane, for low $\tan\beta$. As expected, considerably high values[8] of A, B can generally be achieved for $M_1\simeq M_2$, when $\tan\beta$ is close to 1. Some deviations from the expected behavior in the limit $M_1=M_2$ and $\tan\beta=1$ we treated above are due to our choice $\tan\beta=1.2$. In general, the presence of contour lines that delimit an abrupt change of regime in either A or B generally corresponds to a crossing in the mass ordering of a physically ''pure'' neutralino and a ''mixed'' state (or of two ''pure'' states).

For instance, in Fig. 2, proceeding along the $M_1=M_2$ diagonal from small to large $M_{1,2}$ values, one can single out four different regimes and this can be explained by the discussion above. The behavior of A and B along this diagonal is of particular interest, as anticipated. Indeed, the latter is the only region where A, B can substantially exceed the 0.8 level and the dynamical enhancement mechanism can be fully effective. When $M_{1,2}\lesssim 150$ GeV, the lightest neutralino is an almost pure photino with mass close to $M_{1,2}$ and the next-to-lightest neutralino is a mixed Higgsino–Z-ino state with mass close to Eq. $(8)_+$ (the $+$ refers to the sign considered in the equation). Also, $\widetilde{\chi}_3^0\approx\widetilde{H}_b$ with mass close to $-\mu$, and $\widetilde{\chi}_4^0$ is the other mixed state with mass close to the absolute value of Eq. $(8)_-$. For 150 GeV$\lesssim M_{1,2}\lesssim -\mu=2M_Z$ the mostly $\widetilde{H}_b$ and the lighter mixed states exchange their role, becoming the $\widetilde{\chi}_2^0$ and the $\widetilde{\chi}_3^0$, respectively. This arrangement is then suitable for a dynamical $B(\widetilde{\chi}_2^0\to\widetilde{\chi}_1^0\gamma)$ enhancement with $\widetilde{\chi}_1^0\simeq\widetilde{\gamma}$ and $\widetilde{\chi}_2^0\simeq\widetilde{H}_b$ [cf. Fig. 2(a)]. For $2M_Z\lesssim M_{1,2}\lesssim 200$ GeV, the mass ordering of the dominantly $\widetilde{\gamma}$ and $\widetilde{H}_b$ states is exchanged, but one still has a scenario with dynamical enhancement [cf. Fig. 2(b)]. Note also that the two mixed states exchange their role as well, the one corresponding to the negative mass eigenvalue becoming lighter than the other. This double level crossing actually takes

[8]Note that in the ''democratic'' case $\langle\widetilde{\chi}_i^0|\widetilde{\gamma}\rangle^2=\langle\widetilde{\chi}_i^0|\widetilde{H}_b\rangle^2=1/4$, $i=1, 2$, one would have $A=B=1/16$ only.

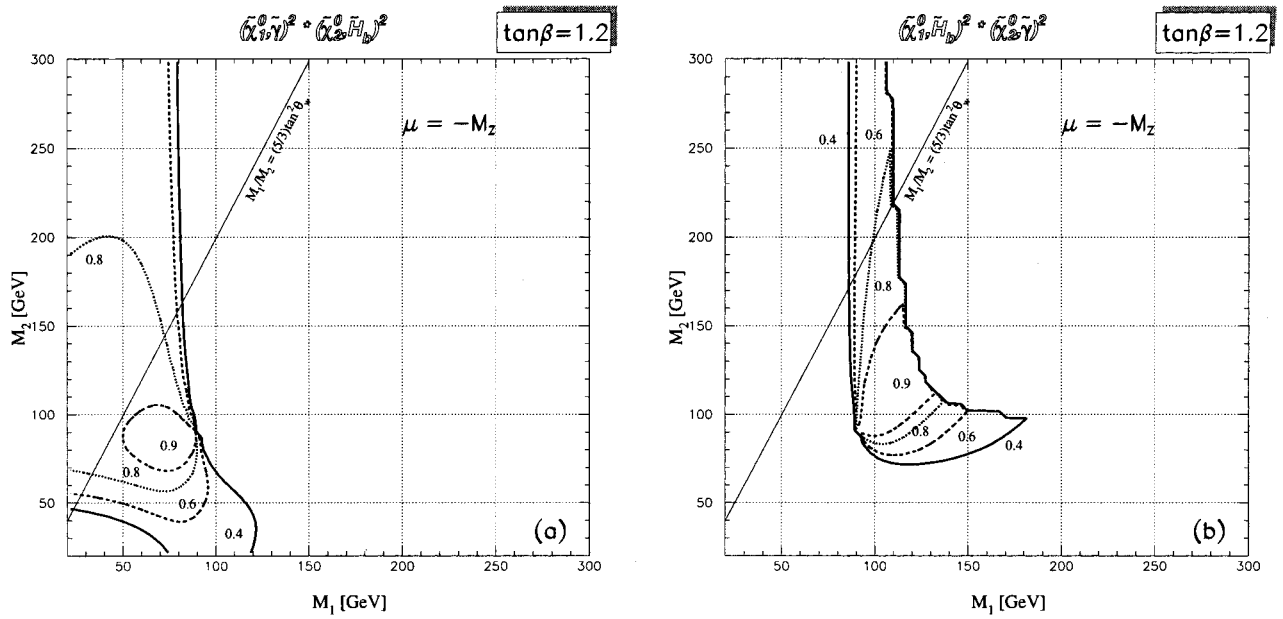

FIG. 3. The same as in Fig. 2, but for $\mu=-M_Z$.

place in the highly degenerate point $M_1=M_2=-\mu\sin2\beta \simeq 179.4$ GeV, where all the contour levels in Fig. 2 tend to crowd. Points of this kind will turn out to be of relevance for the kinematical mechanism too (cf. Sec. IV). Finally, when $M_{1,2}\gtrsim 200$ GeV the negative eigenvalue corresponding to the mixed state crosses the mass level ($\simeq M_{1,2}$) of the almost pure photino, which then becomes the $\widetilde{\chi}_3^0$. Then, the dynamical mechanism stops working, in spite of the presence of an almost pure $\widetilde{H}_b$ as $\widetilde{\chi}_1^0$.

In Fig. 3, we show how the general picture for A and B evolves when μ goes from $-2M_Z$ to $-M_Z$. One can check that the situation is qualitatively similar to the previous case, once the whole structure of the contour plots in the (M_1,M_2) plane is shifted toward the new crossing point $M_1=M_2=-\mu\sin2\beta\simeq 89.7$ GeV. Note, however, that here the quantity A can reach higher values (of order 0.9 or more), and the region where B is large is also wider in Fig. 3 with respect to Fig. 2. Furthermore, it is interesting that it is possible to approach high values of A and B ($A\simeq 0.9$ and $B\simeq 0.85$ in a certain $M_{1,2}$ interval) even in the gaugino-mass unification case.

For $\tan\beta$ as high as 4 (Fig. 4), A and B never reach 0.8 and, consequently, never prompt a sufficient dynamical $B(\widetilde{\chi}_2^0\to\widetilde{\chi}_1^0\gamma)$ enhancement.

IV. KINEMATICAL $\widetilde{\chi}_2^0\to\widetilde{\chi}_1^0\gamma$ ENHANCEMENT

As anticipated in Sec. II, when the contribution of the sfermion exchange to the $\widetilde{\chi}_2^0$ tree-level decays is suppressed (i.e., for heavy scalar masses and/or absence of non-

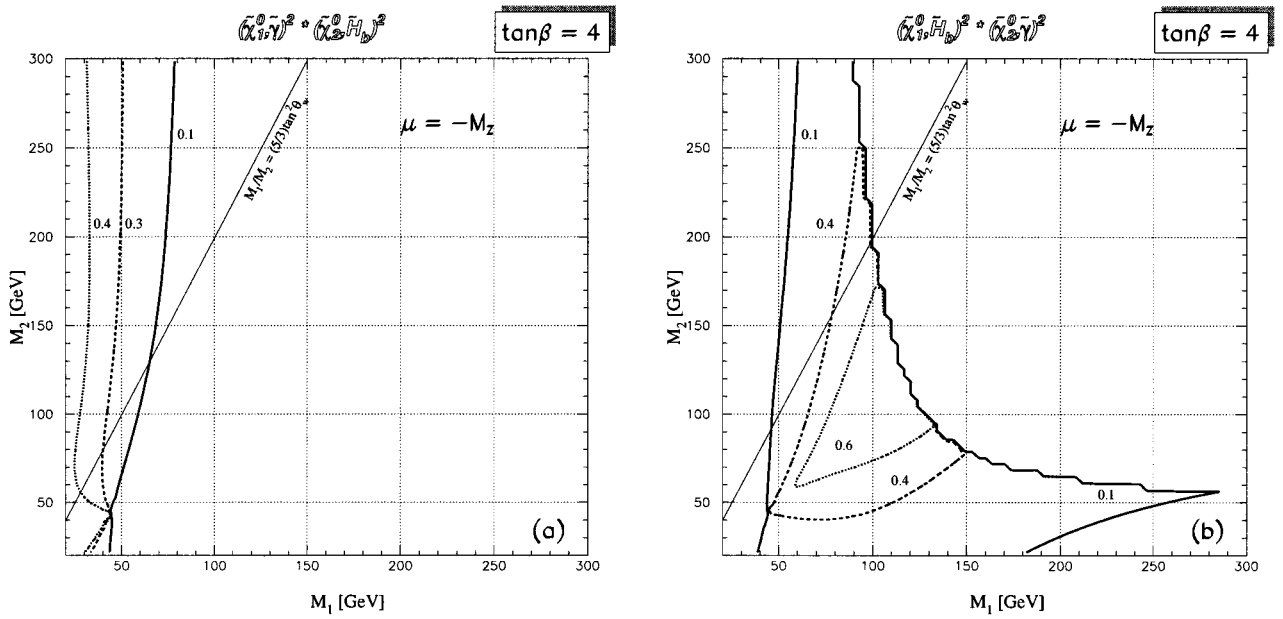

FIG. 4. The same as in Fig. 2, but for $\mu=-M_Z$ and $\tan\beta=4$.

negligible gaugino components in both $\widetilde{\chi}_1^0$ and $\widetilde{\chi}_2^0$), the radiative decay is enhanced by a purely kinematical factor, for almost degenerate $m_{\widetilde{\chi}_1^0}$ and $m_{\widetilde{\chi}_2^0}$. In order to find out where in the SUSY-parameter space the masses of the two lightest neutralinos are almost degenerate, one has to consider the fourth degree eigenvalue equation associated with the neutralino mass matrix (4):

$$0 = m_i^4 + A m_i^3 + B m_i^2 + C m_i + D$$

with

$$A = -\mathrm{Tr}(\mathcal{M}_{\widetilde{\chi}^0}) = -(M_1 + M_2),$$

$$B = M_1 M_2 - \mu^2 - M_Z^2,$$

$$C = \mu^2 (M_1 + M_2) + M_Z^2 (M_1 \cos^2\theta_W + M_2 \sin^2\theta_W - \mu \sin 2\beta),$$

$$D = \det(\mathcal{M}_{\widetilde{\chi}^0}) = \mu [M_Z^2 (M_1 \cos^2\theta_W + M_2 \sin^2\theta_W) \sin 2\beta - \mu M_1 M_2], \tag{13}$$

where m_i $(i=1,...,4)$ is the general neutralino mass eigenvalue. Then, one has to force Eq. (13) (which, arising from a Hermitian, real and symmetric matrix, has four real roots) to have (at least) either two identical roots or two opposite roots, $m_i^0 = \pm m_j^0$ (when using the superscript 0, we generally refer to a degenerate eigenvalue).[9]

Exact expressions for the neutralino masses and mixing can be found in Ref. [25]. Here, we are mainly interested in special cases for which it is possible to extract approximate formulas, more useful for a physical interpretation.

Involving a linear combination of 12-dimensional terms (where up to the 4th power of one of the coefficients A, B, C, D can appear), the general necessary condition to get two identical roots from Eq. (13), seems far too complicated to give any useful information and even to be displayed here. As for the case of two opposite roots, a simple necessary condition in terms of A, B, C, D can be derived

$$A^2 D + A B C + C^2 = 0. \tag{14}$$

Unfortunately, Eq. (14), when translated in terms of M_1, M_2, μ, $\sin 2\beta$, and $\sin^2\theta_w$, turns out to be quite complex too. Thus, in the following, we consider only interesting limits of the SUSY parameters, such as $\tan\beta \to 1$ or $M_1 \to M_2$. Hence, by reducing to zero the off-diagonal terms in one or both of the 2×2 blocks of the matrix (4), one considerably simplifies the eigenvalue Eq. (13) and allows to disentangle the relevant degeneracy scenarios. In this way, we will single out some *sufficient* conditions, which ensure exact or approximate degeneracy between the two lightest neutralino states. This procedure will be supported by an extensive numerical study (scanning the whole SUSY-parameter space) of the relevant mass splitting $(m_{\widetilde{\chi}_2^0} - m_{\widetilde{\chi}_1^0})$, which is shown in the following, as well as a numerical analysis of $B(\widetilde{\chi}_2^0 \to \widetilde{\chi}_1^0 \gamma)$, that we present in the next section. On the basis of the numerical analysis, we found that necessary conditions for an exact degeneracy of the two lightest neutralino states are

$$\tan\beta = 1 \quad \text{or} \quad M_1 = M_2, \tag{15}$$

with the additional requirement $\mu < 0$. The latter directly translates in some *necessary* conditions for a sizable kinematical enhancement of $B(\widetilde{\chi}_2^0 \to \widetilde{\chi}_1^0 \gamma)$. Interestingly enough, these conditions are the same as the ones we found in Sec. III for a dynamical enhancement, although in the latter case, the two conditions on $\tan\beta$ and $M_{1,2}$ have to be fulfilled at the same time. The conditions (15) for a $B(\widetilde{\chi}_2^0 \to \widetilde{\chi}_1^0 \gamma)$ kinematical enhancement are of course interesting only in regions allowed by LEP1–1.5 data. Furthermore, we do not consider here asymptotic regimes with $M_{1,2} \gg M_Z$ and/or $|\mu| \gg M_Z$, or $M_{1,2} \ll M_Z$ and/or $|\mu| \ll M_Z$. Indeed, for instance, the limit $|\mu| \ll M_{1,2}, M_Z$ leads to two almost degenerate Higgsinos-like neutralinos, as discussed above and in Ref. [6]. Other asymptotic cases with possible degeneracy have been mentioned in Sec. II. Here, we will limit our analytical and numerical analyses to the region where $|\mu|$ and $M_{1,2}$ fall both in the interval $[M_Z/4,\ 4M_Z]$.

We stress that here we are interested in the degeneracy of the two lightest neutralinos. This singles out only a few among the possible degeneracy scenarios for the four neutralinos, and makes the analysis more involved.

In order to find *sufficient* conditions for the degeneracy of the two lightest neutralinos, let's now first consider the limit $M_1 = M_2$. Then, it is convenient to solve the Eq. (13) just in terms of M_2 as a function of the generic eigenvalue m_i. For $m_i \neq \pm\mu$, one then gets two branches

$$(M_2)_+ = m_i, \quad (M_2)_- = m_i - M_Z^2 \frac{m_i + \mu \sin 2\beta}{m_i^2 - \mu^2}. \tag{16}$$

Note that the branch $(M_2)_+$ describes the behavior of one neutralino mass eigenvalue only, while the branch $(M_2)_-$ is threefold and corresponds by itself to three generally different eigenvalues. The two main branches $(M_2)_\pm$ intersect in a point (corresponding to a degeneracy with same-sign eigenvalues: $m_{i,j}^0 = M_2$), whenever

$$M_1 = M_2 = -\mu \sin 2\beta. \tag{17}$$

This case is quite interesting. Indeed, one has

$$m_1^0 = m_2^0 = M_1 = M_2 = -\mu \sin 2\beta, \tag{18}$$

$$-m_3^0 = m_4^0 = \sqrt{\mu^2 + M_Z^2}, \tag{19}$$

that is, the two mass eigenvalues with the lower absolute values coincide, while the two eigenvalues with the higher absolute values are opposite. As for the composition, one of the two light degenerate states is a pure photino, while the other is a mixture of $\widetilde{Z}$ and $\widetilde{H}_b$, with $\langle \widetilde{Z} | \widetilde{\chi}_2^0 \rangle^2 = \mu \cos 2\beta / \sqrt{M_Z^2 + \mu^2 \cos 2\beta}$. Thus, the scenario of Eq. (17) is relevant both for the kinematical and for the reduced dynamical enhancement (cf. Sec. II), since the Z^0-exchange contribution to the tree-level decays is highly suppressed. The degeneracy corresponding to Eq. (18) is of course removed when M_1 and M_2 get far apart. Nevertheless, one can check that for

[9] The physical neutralino mass is given by $m_{\widetilde{\chi}_i^0} = |m_i|$.

$(M_1-M_2)\sim 10$ GeV the degeneracy may still be effective for a sizeable kinematical enhancement of the radiative decay.

In principle, one can get other degeneracy scenarios by using Eqs. (16) in different ways, but we will show in the following that they are not relevant for our purposes. First of all, it is clear that the degeneracy between the heavier neutralinos corresponding to Eq. (19) cannot be a direct result of the intersection of the two main branches $(M_2)_\pm$. However, it can happen that two of the three sub-branches of the branch $(M_2)_-$, for a given value of M_2, correspond to two opposite eigenvalues, and hence to degenerate neutralino masses. This is the case when $(m_i^2-\mu^2)=M_Z^2$, which is nothing but the degeneracy (19). The additional fact that in such a scenario one necessarily has also $M_2=-\mu\sin 2\beta$ [corresponding to a *real* intersection of the two main branches $(M_2)_\pm$ and to the further degeneracy (18) of two always lighter neutralino states] makes the above circumstance negligible for us here. One can look for other cases of degeneracy by considering the possibility that one of the eigenvalues described by the branch $(M_2)_-$ has the same absolute value of the one corresponding to the branch $(M_2)_+$, but opposite sign. This corresponds to solving the equation

$$M_Z^2\,\frac{M_2-\mu\,\sin 2\beta}{M_2^2-\mu^2}-2M_2=0, \tag{20}$$

while, for the two degenerate eigenvalues, one has: $m_i^0=-m_j^0=M_1=M_2$. The solutions of Eq. (20) are in general complicated expressions, but one can easily find them numerically. After such an analysis, we did not encounter any further case of exact neutralino mass degeneracy from Eq. (20) in the limit $(M_1-M_2)\to 0$ relevant for the kinematical enhancement, in regions allowed by the LEP data.

Relaxing the limit $M_1=M_2$, a different necessary condition to get mass degeneracy in Eq. (13) is, indeed, $\tan\beta\to 1$. In this limit, contrary to the previous case, the easiest part of the neutralino mass matrix is the Higgsino sector. Then, we can solve the eigenvalue equation with respect to μ as a function of m_i, in order to get other *sufficient* conditions, and scenarios of interest for the kinematical enhancement. One then finds again two branches

$$(\mu)_-=-m_i,$$

$$(\mu)_+=m_i-M_Z^2\,\frac{m_i-M_1\cos^2\theta_W-M_2\,\sin^2\theta_W}{(m_i-M_1)(m_i-M_2)}, \tag{21}$$

where, similarly to the case of Eqs. (16), the branch $(\mu)_-$ describes a single neutralino mass eigenvalue and the branch $(\mu)_+$ corresponds to three different eigenvalues. Note that here, contrary (and complementary) to the case of Eq. (16), one can have $m_i=\pm\mu$, but not $m_i=M_1$ or M_2. By using Eqs. (21), one can single out degeneracy scenarios with $m_i^0=\pm m_j^0=\mu$. In order to realize the case with two same-sign degenerate eigenvalues, the general condition

$$M_Z^2\,\frac{\mu+M_1\cos^2\theta_W+M_2\sin^2\theta_W}{(\mu+M_1)(\mu+M_2)}-2\mu=0, \tag{22}$$

must hold. Again, the corresponding explicit solutions are rather complex, but one can solve Eq. (22) numerically to find the regions of the parameter space interesting for the kinematical enhancement. Since, in contrast to the case of Eq. (20), Eq. (22) gives rise to interesting scenarios, it is useful to consider here, in addition to $\tan\beta\to 1$, the special limit $\sin^2\theta_W=0$, which allows a simplified analytical treatment. Indeed, in this way, two free gaugino mass parameters are still present, but the mixing in the gaugino sector disappears. Furthermore, this limit is not too far away from the real physical case $\sin^2\theta_W\simeq 0.23$. Equation (22) gives then the solutions (when $\tan\beta=1$)

$$m_i^0=m_j^0=-\mu=\frac{1}{2}\,(M_2\mp\sqrt{M_2^2+2M_Z^2}). \tag{23}$$

The existence of the solutions (23) (not their exact form), is independent of the limit $\sin^2\theta_W\to 0$ and the corresponding exact degeneracy is removed only for $\tan\beta\neq 1$. The introduction of this limit allows us to disentangle two other interesting cases, as long as $\tan\beta=1$, that is

$$m_i^0=m_j^0=-\mu=M_1, \tag{24}$$

and, when the condition

$$M_1-\frac{M_Z^2}{M_1-M_2}-\mu=0 \tag{25}$$

is fulfilled,

$$m_i^0=m_j^0=M_1=\mu-\frac{M_Z^2}{M_1-M_2}. \tag{26}$$

The latter cases, needing $m_i=M_1$, cannot be directly derived from the two branches in Eq. (21). The correct procedure to get them is to solve the eigenvalue equation with respect to μ or M_1, by applying both the limits $\tan\beta\to 1$ and $\sin^2\theta_W\to 0$ simultaneously.

In order to understand the nature of these additional solutions and their link with the limit $\sin^2\theta_W\to 0$, some further explanation is needed. A solution corresponding to Eq. (24) survives when $\sin^2\theta_W\neq 0$, although the expression for the degenerate mass eigenvalues receives some corrections, as in the case of solutions (23). What makes case (24) different from the previous ones is that the corresponding degeneracy is not removed when $\tan\beta$ goes away from 1 and both $\sin^2\theta_W\neq 0$ and $\tan\beta\neq 1$ are needed to do the job. In this sense, the degeneracy corresponding to Eq. (24) is more *solid* than the others. As for solution (26), instead, it represents a spurious case which does not correspond anymore to an exact degeneracy when $\sin^2\theta_W\neq 0$, but only to a case where two neutralino mass eigenvalues are close to each other (in the limit $\tan\beta\to 1$), although not quite equal. To get an effective kinematical $B(\widetilde{\chi}_2^0\to\widetilde{\chi}_1^0\gamma)$ enhancement, we are interested in scenarios where neutralino mass differences of order 10 GeV or less arise. In order to obtain such a small $(m_i^0-m_j^0)$ when Eq. (26) holds, one needs M_1, $M_2\ll M_Z$, $|\mu|$, with $|\mu|\approx$TeV [because of condition (25)]. Then, the quantity $(M_1\cos^2\theta_W+M_2\sin^2\theta_W)$ in Eq. (13) can be treated in the same way as it would be in the limit $\sin^2\theta_W\to 0$. Therefore, we will neglect this possibility (corresponding to an asymptotic case, already excluded by LEP) and we will focus on solutions (23), (24).

We stress that the existence of the solutions (23), (24) (not the exact expression for the degenerate eigenvalues) is independent of the limit $\sin^2\theta_W \to 0$ and the corresponding exact degeneracy is removed only for $\tan\beta \neq 1$. Anyway, the simplified solutions we found allow us to emphasize some remarkable properties which remain valid with a good approximation for $\sin^2\theta_W \simeq 0.23$ (and, often, even for $\tan\beta \simeq 1$, rather than exactly 1). For instance, the solutions corresponding to $(23)_+$ and (24) are only possible for negative values of μ [even $\mu < -M_Z/\sqrt{2}$ in the case $(23)_+$].[10] In contrast, the solution $(23)_-$ is allowed only for $0 \leqslant \mu \leqslant M_Z/\sqrt{2}$ (that is in a region that, particularly for small $\tan\beta$, is excluded by LEP1–1.5 data, due to the presence of a light chargino). Hence, solution $(23)_-$ will not play an important role in the following discussions. Also, note that the solution (24) is present irrespective of the particular value of M_2 and, similarly, the solutions (23) do not depend on M_1, in the limit $\tan\beta \to 1$, $\sin^2\theta_W \to 0$ and exact degeneracy. For $\sin^2\theta_W \simeq 0.23$, the solution (23) [(24)] develops a weak dependence on M_1 [M_2], as will be shown in the following numerical study.

As for the limit $\tan\beta \to 1$, up to now we only took care of deriving some sufficient conditions for the degeneracy of any pair of neutralinos. Now, we need to check when the degeneracy scenarios we singled out actually concern the two lightest neutralino mass eigenstates. We will focus on the more interesting scenarios $(23)_+$ and (24). Which pair of mass eigenstates is involved in the degeneracy depends also on the parameters not directly entering the approximate conditions (23), (24), in a generally simple way. For a given value of $|\mu|$, typically one observes that, for $M_1[M_2] > |\mu|$, the degeneracy of the kind $(23)_+$ [(24)] indeed concerns the two lightest neutralino states. On the other hand, as long as $M_1[M_2] < |\mu|$, the solution for the mass degeneracy corresponds to $m_{\tilde{\chi}^0_2} = m_{\tilde{\chi}^0_3} = -\mu$ and, thus, does not give rise to any kinematical suppression.

All the $\tan\beta = 1$ scenarios above are derived by forcing the two branches in Eqs. (21) to meet in a point of the (m_i, μ) plane, corresponding to a *strict* degeneracy $m^0_i = m^0_j$. However, as done above in the limit $(M_1 - M_2) \to 0$ with Eq. (20), here too we must take into account the additional possibility of a degeneracy with opposite eigenvalues $m^0_i = -m^0_j$. Imposing the corresponding condition $(\mu)_+ = -(\mu)_-$ in Eqs. (21) leads to the interesting case

$$m^0_i = -m^0_j = \mu = M_1 \cos^2\theta_W + M_2 \sin^2\theta_W, \qquad (27)$$

which satisfies the Eq. (14) and is only realized for positive values of μ. This gives rise to a scenario where a pure $\widetilde{H}_b$ is degenerate with a superposition of the other interaction eigenstates. The other two neutralinos are mixed $\widetilde{\gamma}$-$\widetilde{Z}$-$\widetilde{H}_a$ states too, and correspond to the mass eigenvalues

$$m^{(\pm)}_{\widetilde{\gamma}\text{-}\widetilde{Z}\text{-}\widetilde{H}_a} = \frac{1}{2}\left[M_1 + M_2 \pm \sqrt{(M_1 - M_2)^2 + 4M_Z^2}\right]. \qquad (28)$$

On the other hand, the degeneracy must involve the two lightest states. It is easy to show with analytical arguments that this can never happen in regions allowed by LEP1–1.5 data. Hence, the scenario of Eq. (28) is not relevant for the radiative neutralino decay.

Finally, it is interesting to note that in the limit where both $\tan\beta \to 1$ and $(M_1 - M_2) \to 0$, both the kinematical and the dynamical enhancements can be optimized at the same time in the special point $M_1 (= M_2) = -\mu$, where the two lightest neutralinos are always a pure $\widetilde{\gamma}$ and a pure $\widetilde{H}_b$ [cf. Sec. III, Eqs. (8) and Eqs. (18), (19)]. We will see, in the numerical analysis of Sec. V, that a considerably wide region of the SUSY-parameter space where high $B(\widetilde{\chi}^0_2 \to \widetilde{\chi}^0_1 \gamma)$ values are realized is centered on this highly degenerate point.

As for the kinematical enhancement, by using numerical methods, we did not find any other clear case of $\widetilde{\chi}^0_1$-$\widetilde{\chi}^0_2$ exact mass degeneracy, besides the ones we have described above. Also, it was not possible to achieve an approximate degeneracy (at the level of a 10 GeV mass difference) either, in regions of the SUSY space where the *necessary* conditions (15) are rather far from being valid. This does not mean we listed all the possibilities for neutralino mass degeneracy. For instance, one can consider the case $D = \det(\mathcal{M}_{\tilde{\chi}^0}) = 0$. This can be achieved either when $\mu = 0$ and/or $M_{1,2} = 0$, or whenever Eq. (11) holds. The first option was already considered among the asymptotic cases. In the second case, one is left with a simplified eigenvalue equation, which gives rise to other degeneracy scenarios.[11] However, these scenarios always give rise also to at least a null mass eigenvalue; hence, the degeneracy can only concern the $\widetilde{\chi}^0_2$ and the $\widetilde{\chi}^0_3$ or the $\widetilde{\chi}^0_3$ and the $\widetilde{\chi}^0_4$. Other complex degeneracy scenarios, not of interest here, can be constructed.

In summary, the relevant approximate scenarios for the $B(\widetilde{\chi}^0_2 \to \widetilde{\chi}^0_1 \gamma)$ kinematical enhancement are given, for $\mu < 0$, by Eq. (18), when $M_1 \simeq M_2$, and by Eqs. $(23)_+$ and (24), when $\tan\beta \simeq 1$. In order to get a clear picture of the nontrivial behavior of the neutralino mass degeneracy, we now show a set of contour plots for the two lightest neutralino mass difference $(m_{\tilde{\chi}^0_2} - m_{\tilde{\chi}^0_1})$ in the (M_1, M_2) plane, for different values of μ and $\tan\beta$.

In Fig. 5, the case $\mu = -2M_Z$ is shown for $\tan\beta = 1.2$ (a) and 4 (b). The line corresponding to the gaugino mass unification is also plotted. The general pattern is highly nontrivial and quite dependent on $\tan\beta$. In Fig. 5(a), one can easily note the presence of two quite narrow bands, a vertical one and a horizontal one. The horizontal one corresponds to the region where the degeneracy scenario of Eq. $(23)_+$ is approximatively realized for $\tan\beta$ close to 1 and is well outlined by the 15-GeV mass-difference contour. As anticipated, the band is there only for $M_1 \gtrsim -\mu = 2M_Z$ and shows only a weak dependence on M_1. Indeed, by solving numerically Eq. (22) for the general condition of degeneracy, we found that the contour line of exact $m^0_1 = m^0_2$ degeneracy, in the limit $\tan\beta = 1$, passes through the points $(M_1, M_2) = (200, 168.9)$; (250, 166.2); (300, 165.7) GeV, showing a small dependence on M_1 due to the finite value of $\sin^2\theta_W$.

[10] The subscript $\pm$ of the equation number picks out one of the two possible signs in Eq. (23).

[11] For instance, one finds a nontrivial degeneracy, for a given value of $\tan\beta$, in the case $M_1 = M_2 = (M_Z/2)(1 + \sqrt{1 + 8\sin^2 2\beta})^{1/2}$ and $\mu = (M_Z/\sqrt{2})(\sqrt{1 + 8\sin^2 2\beta} - 1)^{1/2}$. The corresponding degenerate neutralinos are $\widetilde{\chi}^0_2$ and $\widetilde{\chi}^0_3$, with opposite mass eigenvalues.

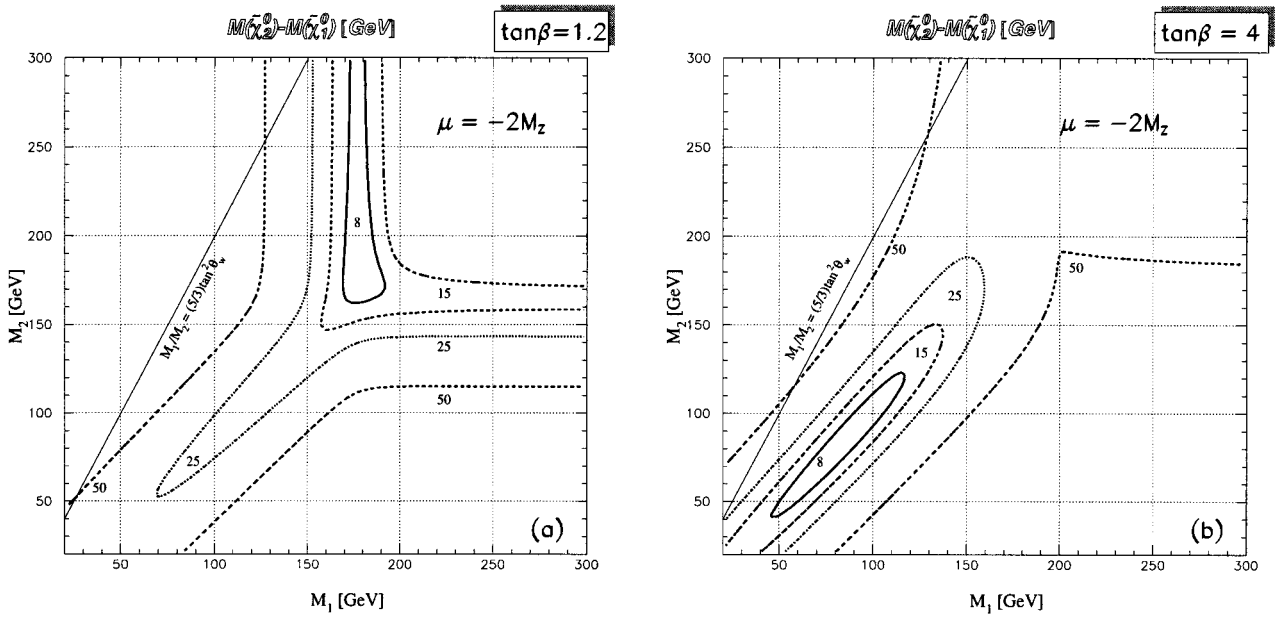

FIG. 5. Contour plot for the difference (in GeV) between the two lightest neutralino masses in the (M_1, M_2) plane for $\mu=-2M_Z$, and $\tan\beta=1.2$ (a) and 4 (b). Different levels are represented by lines of different style. The straight line corresponding to the gaugino mass unification is also shown.

Note that the same equation indicates the presence of a degeneracy also for $M_2=163.7$ and 161.5 GeV, respectively, for $M_1=100$ and 150 GeV, but this corresponds to a case with $m_2^0=m_3^0$, which of course does not show on the figure and is not interesting here. The vertical band, well outlined by the 8 and 15 GeV contours, represents the degeneracy (24). Again, the band is present only for $M_2 \gtrsim 2M_Z$ and has only a weak dependence on M_2, depending on the finite value of $\sin^2\theta_W$. The contour line of exact degeneracy passes now through the points $(M_1, M_2)=(179.7, 200)$; (178.2, 250); (177.7, 300) GeV. Again, there is also a degeneracy concerning $\tilde{\chi}_2^0$ and $\tilde{\chi}_3^0$ when $M_1=175.7$ and 170.9 GeV, respectively, for $M_2=100$ and 150 GeV.

Two additional remarks are in order. First, the vertical band of scenario (24) is clearer and corresponds to a higher degree of degeneracy. This was explained above, in connection with the relation of this scenario with the limit $\sin^2\theta_W \to 0$. Second, both the 8 GeV and the 15 GeV contour have a bulge where they change direction, along the diagonal, towards lower values of M_1 and M_2. Even more visible is this effect if one observes the 25 GeV contour. This corresponds to the region around the point in the (M_1, M_2) plane where the further case of $m_1^0=m_2^0$ degeneracy we singled out is realized. This is given by Eq. (18), that, in the special case $\tan\beta=1.2$, gives $M_1 \simeq M_2 \simeq -\mu \sin 2\beta = 179.4$. Some degeneracy is still present along the diagonal $M_1=M_2$, to the left and below the highly degenerate region $M_1 \simeq M_2 \simeq -\mu$, although to a minor degree than in the horizontal and vertical bands. The degeneracy scenario (18) is more crucial in Fig. 5(b), where $\tan\beta$ is far away from 1 and the other degeneracy scenarios cannot be realized. Here the 8, 15, and 25 GeV contours surround the degeneracy point $M_1=M_2=-\mu \sin 2\beta = 85.8$ GeV and extend along the $M_1=M_2$ diagonal in both the directions. Furthermore, note that this point corresponds to a case of exact degeneracy, while the ''median'' lines of the horizontal and vertical bands in Fig. 5(a) do not, since $\tan\beta$ is only approximately equal to 1. It is useful to check that the vertical line of approximate degeneracy [see, for instance, the one for $M_1 \simeq 175$–180 GeV in Fig. 5(a)] is directly related to the mass-level crossing of two slightly mixed lightest neutralinos along the same line (see, for instance, the behavior of A and B in Fig. 2).

We will see in the next section that the degeneracy along the $M_1=M_2$ diagonal will translate in explicit effects on $B(\tilde{\chi}_2^0 \to \tilde{\chi}_1^0 \gamma)$ for $\tan\beta$ well above 1, while, in the low $\tan\beta$ case, they will be mixed with and partly hidden by the dynamical enhancement. A final comment on Fig. 5 is about the gaugino mass unification. We can see that is not possible in the unified case to realize a $\tilde{\chi}_1^0 - \tilde{\chi}_2^0$ mass approximate degeneracy at a level of less than 25 GeV mass difference, unless $M_2 \gtrsim 300$ GeV and $\tan\beta$ is small (apart from the very low $M_{1,2}$ region).

Figure 6 shows how the general picture evolves when μ goes from $-2M_Z$ to $-M_Z$. The behavior of $(m_{\tilde{\chi}_2^0} - m_{\tilde{\chi}_1^0})$ is qualitatively similar to the previous case, although the regions of strong degeneracy are shifted towards lower values of $M_{1,2}$.

Before coming to the numerical study of $B(\tilde{\chi}_2^0 \to \tilde{\chi}_1^0 \gamma)$, it is useful to note that the dynamical and kinematical mechanism can be present at the same time in special cases and work together to enhance $B(\tilde{\chi}_2^0 \to \tilde{\chi}_1^0 \gamma)$. For instance, a moderate degeneracy is needed between $m_{\tilde{\chi}_1^0}$ and $m_{\tilde{\chi}_2^0}$ for the kinematical mechanism to be effective, when $\tilde{\chi}_1^0$ and $\tilde{\chi}_2^0$ also have a definite different composition and vice versa. Also note that the general necessary conditions (i.e., $\tan\beta \simeq 1$, $M_1 \simeq M_2$, with $\mu<0$) are the same for both mechanisms, and this strengthens the enhancement effect.

V. NUMERICAL ANALYSIS OF $B(\tilde{\chi}_2^0 \to \tilde{\chi}_1^0 \gamma)$

On the basis of the results presented in Secs. III and IV on the enhancement regimes for the radiative $\tilde{\chi}_2^0$ decay, we are

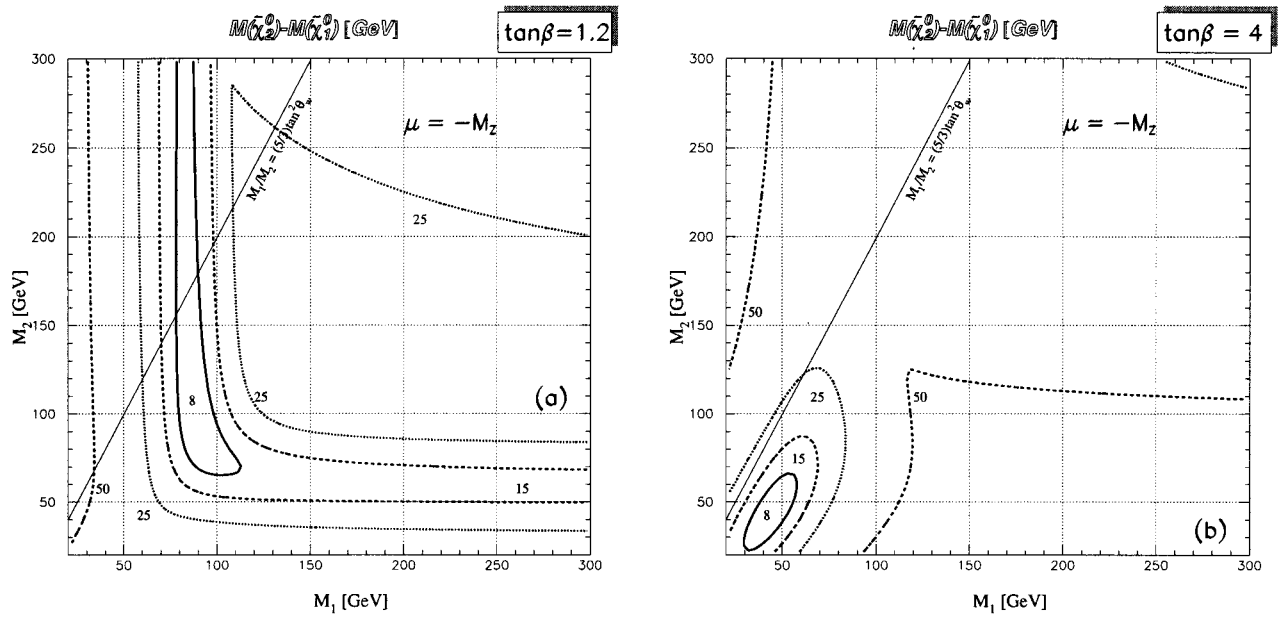

FIG. 6. The same as in Fig. 5, but for $\mu=-M_Z$.

now ready to explain the nontrivial behavior of the corresponding BR in the SUSY parameter space. One of the main findings will be the existence of significant regions of this space, of interest for collider physics, where $\tilde{\chi}_2^0\to\tilde{\chi}_1^0\gamma$ is the dominant $\tilde{\chi}_2^0$ decay. Following the previous discussion, we present the $B(\tilde{\chi}_2^0\to\tilde{\chi}_1^0\gamma)$ in the (M_1,M_2) plane, for fixed values of $\tan\beta$ and μ. We also discuss the BR dependence on the scalar masses.

First of all, one has to set the parameter regions already excluded by the experimental search. We recall that the usual analysis implies the condition $M_1/M_2=(5/3)\tan^2\theta_W$. Relaxing the latter, the definition of the exclusion regions gets of course more involved. We considered the following bounds from LEP1 data on the Z^0 line shape and on neutralino direct searches [19,21,20]:

$$\Gamma_{\rm tot}(Z^0\to{\rm SUSY})<23\ \ {\rm MeV},$$

$$\Gamma_{\rm inv}(Z^0\to{\rm SUSY})<5.7\ \ {\rm MeV},$$

$$B(Z^0\to\tilde{\chi}_1^0\tilde{\chi}_2^0)<3.9\times10^{-6},$$

$$B(Z^0\to\tilde{\chi}_2^0\tilde{\chi}_2^0)<3.9\times10^{-6},$$

where we took into account not only the $\tilde{\chi}_1^0\tilde{\chi}_1^0$ contribution to the Z^0 invisible width, but all the channels $Z^0\to\tilde{\chi}_i^0\tilde{\chi}_j^0$, $i,j=1,...,4$, with following invisible decays of the produced heavier neutralinos $\tilde{\chi}_i^0\to\tilde{\chi}_1^0\nu\overline{\nu}(...\nu\overline{\nu})$.

As for LEP1.5, we imposed the following limits from the direct searches of neutralinos/charginos during the runs at $\sqrt{s}=130.3$ and 136.3 GeV [26]

$$\sigma_{\rm vis}\left[e^+e^-\to\sum_{i,j}\ (\tilde{\chi}_i^0\tilde{\chi}_j^0,\tilde{\chi}_i^+\tilde{\chi}_j^-)\right]<2\ \ {\rm pb}$$

at

$$\sqrt{s}=130.3\ \ {\rm GeV},$$

if

$$(m_{\tilde{\chi}_2^0}-m_{\tilde{\chi}_1^0})\ \ {\rm or}\ \ (m_{\tilde{\chi}_1^\pm}-m_{\tilde{\chi}_1^0})>10\ \ {\rm GeV},$$

$$\sigma_{\rm vis}\left[e^+e^-\to\sum_{i,j}\ (\tilde{\chi}_i^0\tilde{\chi}_j^0,\tilde{\chi}_i^+\tilde{\chi}_j^-)\right]<2.4\ \ {\rm pb}$$

at

$$\sqrt{s}=136.3\ \ {\rm GeV},$$

if

$$(m_{\tilde{\chi}_2^0}-m_{\tilde{\chi}_1^0})\ \ {\rm or}\ \ (m_{\tilde{\chi}_1^\pm}-m_{\tilde{\chi}_1^0})>10\ \ {\rm GeV},$$

which corresponds to not allowing more than ten total visible events from neutralino/chargino production at LEP1.5. Here too, the branching fractions into visible final states of the produced particles have been taken into account while computing $\sigma_{\rm vis}$. The above LEP1.5 limits translate into an approximate bound on the chargino mass $m_{\tilde{\chi}_1^\pm}\gtrsim65$ GeV, when the sneutrino mass is not too light $[m(\tilde{\nu})\gtrsim200$ GeV] and there is enough phase space available to ensure the presence of rather energetic particles among the chargino decay products: $(m_{\tilde{\chi}_1^\pm}-m_{\tilde{\chi}_1^0})>10$ GeV.

A few comments are in order. By applying the above experimental constraints, one finds that for rather small values of $\tan\beta$ and $0\lesssim\mu\lesssim M_Z$ wide regions in the plane (M_1,M_2) are excluded. For instance, at $\tan\beta=1.2$ and $\mu=M_Z$, the area with $M_1,M_2\lesssim180$ GeV is forbidden. The regions with positive μ are, however, not much relevant for the radiative $\tilde{\chi}_2^0$ decay, as we know from Secs. III and IV. For low $\tan\beta$, negative μ and small $|\mu|$ (around 50 GeV) one gets highly nontrivial exclusion regions (see below). On the other hand, whenever the chargino search turns out to be the most effective means of constraining the plane (M_1,M_2), the mass limit and the forbidden region tend to get indepen-

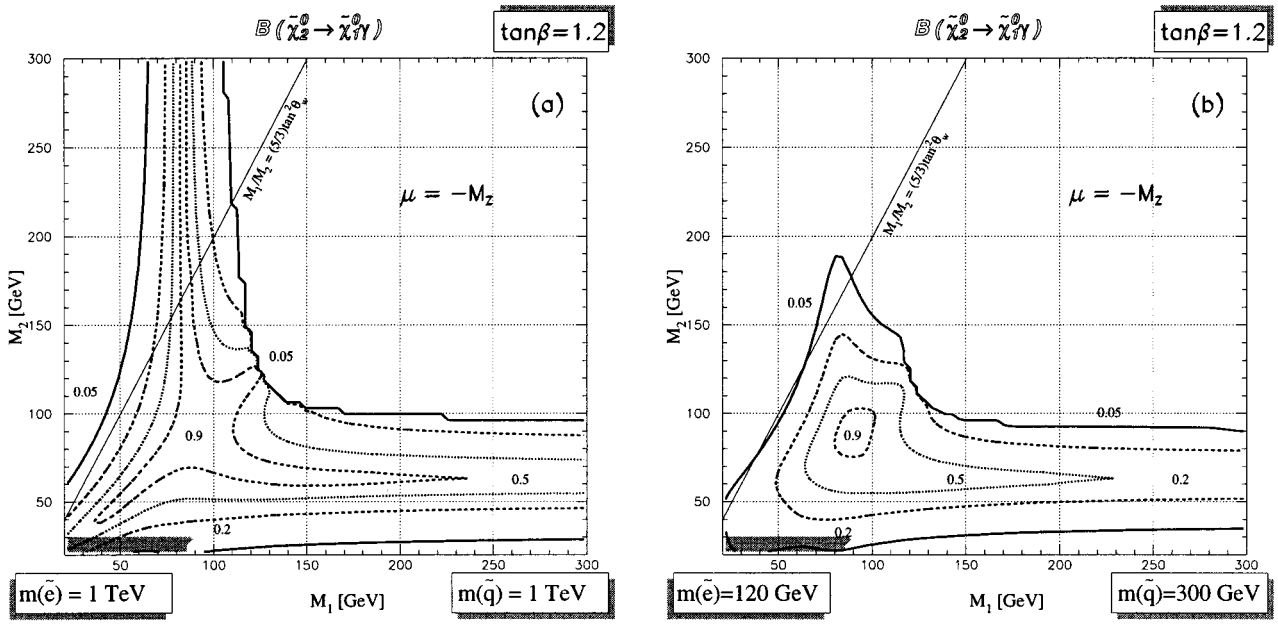

FIG. 7. Contour plot for the branching ratio of the neutralino radiative decay. In (a), all the sfermions are taken degenerate with mass equal to 1 TeV. In (b), the left and right charged slepton masses are taken degenerate and equal to 120 GeV; the sneutrino mass is calculated by using the SU(2) sum rule; the squark masses are taken all degenerate and equal to 300 GeV. The Higgs sector masses and couplings are set by $m_A=300$ GeV. The shaded region is excluded by LEP1 and LEP1.5 data.

dent of M_1. The possible relevance of neutralino searches can translate, instead, in more involved bounds, depending on M_1.

In Fig. 7, we show the $B(\widetilde{\chi}_2^0\to\widetilde{\chi}_1^0\gamma)$ for $\tan\beta=1.2$ and $\mu=-M_Z$, i.e., in a regime where both the dynamical and kinematical enhancement can be realized. The shaded region is excluded by LEP1–1.5 data. In this figure and in all the following ones, we calculate the Higgs sector masses and couplings by assuming $m_A=300$ GeV. In Fig. 7(a), the kinematical enhancement is optimized by the large value (1 TeV) assumed for the sfermion masses. We find a significant area in the plane (M_1,M_2) where $B(\widetilde{\chi}_2^0\to\widetilde{\chi}_1^0\gamma)>90\%$. Its shape can be straightforwardly explained by putting together the information from Fig. 3, on the physical purity of the two lightest neutralinos, and Fig. 6(a), on the neutralino mass degeneracy. It is interesting to note in Fig. 7(a) how much, along the $M_1\simeq M_2$ diagonal, different enhancement mechanisms can be effective and can contribute to a large $B(\widetilde{\chi}_2^0\to\widetilde{\chi}_1^0\gamma)\gtrsim 90\%$, depending on the $M_{1,2}$ values. For instance, when $M_1\simeq M_2\simeq 40$ GeV, the two lightest neutralinos have widely different masses [cf. Fig. 6(a)] and the kinematical enhancement is not operative. Furthermore, since $\tan\beta$ is not exactly 1, $\widetilde{\chi}_2^0$ has comparable $\widetilde{Z}$ and $\widetilde{H}_b$ components, spoiling the full dynamical enhancement. However, since the sfermions are very heavy, it is sufficient the presence of a nearly pure $\widetilde{\chi}_1^0\simeq\widetilde{\gamma}$ to largely deplete the only tree-level decay channel left (through Z^0 exchange) and to give rise to very large $B(\widetilde{\chi}_2^0\to\widetilde{\chi}_1^0\gamma)$ values (*reduced* dynamical suppression, cf. Sec. II). Of course, after lowering the sfermion masses this enhancement regime does not survive [cf. Fig. 7(b)]. Proceeding towards higher $M_{1,2}\simeq-\mu\sin 2\beta$ values on the diagonal, one has two enhancement mechanisms getting effective at the same time. First, the $\widetilde{H}_b$ component of the $\widetilde{\chi}_2^0$ grows [cf. Fig. 3(a)], giving rise to a ''full'' dynamical enhancement. Second, $m_{\widetilde{\chi}_1^0}$ and $m_{\widetilde{\chi}_2^0}$ get closer and closer [cf. Fig. 6(a)] and the kinematical mechanism becomes effective as well. The most favorable situation is then realized in this region. For larger values of $M_{1,2}$ in the [100, 120] GeV range, the dynamical enhancement dominates, but with $\widetilde{\chi}_1^0\simeq\widetilde{H}_b$ and $\widetilde{\chi}_2^0\simeq\widetilde{\gamma}$ [cf. Fig. 3(b)]. Finally, when M_1 and M_2 are both $\gtrsim$120 GeV, large $B(\widetilde{\chi}_2^0\to\widetilde{\chi}_1^0\gamma)$ values cannot be achieved anymore.

The relative importance of the various kinematical enhancement scenarios can be guessed by comparing Fig. 7(a) with Fig. 7(b). In the latter, lighter scalars, that tend to reduce the effect of the kinematical suppression in the $\widetilde{\chi}_2^0$ tree-level decays, are assumed. Nevertheless, a strong radiative enhancement mainly due to a dynamical suppression of the tree-level decays is still present for $M_1\simeq M_2\simeq-\mu$. Note that the kinematical enhancement which is expected from the scenario $(23)_+$ [cf. the horizontal band of approximate degeneracy in Fig. 6(a)] is only slightly influenced by the change of the sfermion mass values, while the scenario (24) (vertical band) corresponds to higher values of $B(\widetilde{\chi}_2^0\to\widetilde{\chi}_1^0\gamma)$ for heavy sfermion masses, and is much more sensitive when changing these parameters. This happens in spite of the greater degree of neutralino mass degeneracy corresponding to the scenario (24). The reason is that in the case (23), in addition to the kinematical suppression of the tree-level decay widths, one has a rather large value of the radiative decay width, due to the presence of light charginos (low M_2) in the $W^\pm/\widetilde{\chi}^\mp$ loops, irrespective of the sfermion masses. For instance, the point $M_1=180$ GeV, $M_2=60$ GeV in Fig. 7(a) corresponds to a total $\widetilde{\chi}_2^0$ decay width of about 100 eV and only about 5% of it is due to tree-level decays (in particular, cascade decays with $m_{\widetilde{\chi}_2^0}=97$ GeV, $m_{\widetilde{\chi}_1^\pm}=93$ GeV, and $m_{\widetilde{\chi}_1^0}=85$ GeV). In contrast, in the ''unified'' point $M_1=85.2$ GeV, $M_2=170$ GeV, one has $\Gamma_{\rm tot}(\widetilde{\chi}_2^0)\simeq\Gamma(\widetilde{\chi}_2^0\to\widetilde{\chi}_1^0\gamma)\sim 1$ eV for 1 TeV sfermion masses, while the total $\widetilde{\chi}_2^0$ width ap-

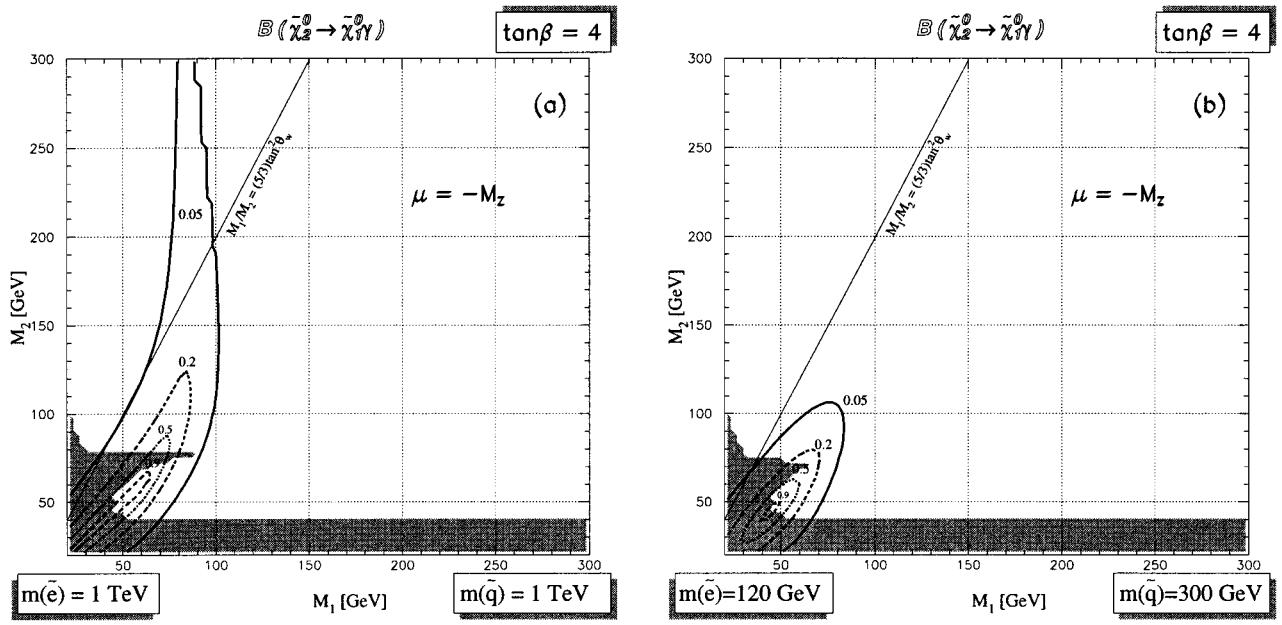

FIG. 8. The same as in Fig. 7, but for tanβ=4.

proaches 50 eV for the lighter sfermion masses used in Fig. 7(b), about 90% of it coming from tree-level light-slepton exchange channels.

A final remark on Fig. 7 is that there are regions where neither the kinematical nor the dynamical $B(\widetilde{\chi}_2^0 \to \widetilde{\chi}_1^0 \gamma)$ enhancements are fully effective, since the regimes for the SUSY parameters we outlined in Secs. III and IV are only realized with a large approximation. Nevertheless, the combined effect of the two mechanisms can still give rise to large values of $B(\widetilde{\chi}_2^0 \to \widetilde{\chi}_1^0 \gamma)$.

When tanβ rises (for instance, tanβ=4 is assumed in Fig. 8) the physical *purity* of neutralinos decreases (see the corresponding Fig. 4), and mainly effects connected to the kinematical enhancement in the scenario (18) survive. This can be easily verified by comparing Fig. 8 with Fig. 6(b). The value of the sfermion masses is then a relevant parameter. Assuming lighter scalars [Fig. 8(b)] considerably reduces the region of large radiative BR with respect to the regime where the sfermion exchange in the tree-level $\widetilde{\chi}_2^0$ decay is suppressed by heavy scalars [Fig. 8(a)].

We consider now the effect of varying the parameter μ. From now on, we will keep the sfermion masses rather heavy [i.e., we set $m(\widetilde{e})=m(\widetilde{q})=1$ TeV] in order to optimize the $B(\widetilde{\chi}_2^0 \to \widetilde{\chi}_1^0 \gamma)$ enhancement. In Fig. 9, the effect of decreasing μ down to $-2M_Z$ is shown for tanβ=1.2.

Again, some insight of the BR behavior can be gained by looking back at Fig. 2 (physical ''purity'' of the neutralinos) and Fig. 5(a) (neutralino mass degeneracy). The area around $M_1 \simeq M_2 \simeq -\mu$ is again particularly promising. However, quite large radiative BR's can be also achieved in three strips of the (M_1, M_2) plane, corresponding to different kinematical enhancement scenarios [cf. Fig. 5(a)]. Some effects from the *reduced* dynamical mechanism with heavy sfermion masses are also present.

Keeping μ in the negative range, we now go to larger μ values, which are of particular interest for explaining the $e^+e^-\gamma\gamma+\not{E}_T$ event at the Tevatron. In Figs. 10(a) and 10(b), the results for $\mu=-55$ GeV at tanβ=1.2 and 2, respectively, are shown. While a large $B(\widetilde{\chi}_2^0 \to \widetilde{\chi}_1^0 \gamma)$ can still be obtained comfortably, we can observe that for increasing tanβ the regions excluded by present data extend further and further.

Going to $\mu=-M_Z/2$ at tanβ=1.2 (cf. Fig. 11) has the effect of a moderate shifting of the large BR regions down to smaller M_1, M_2 with respect to Fig. 10(a), accompanied again by a drastic reduction of the parameter space allowed by the experimental data.

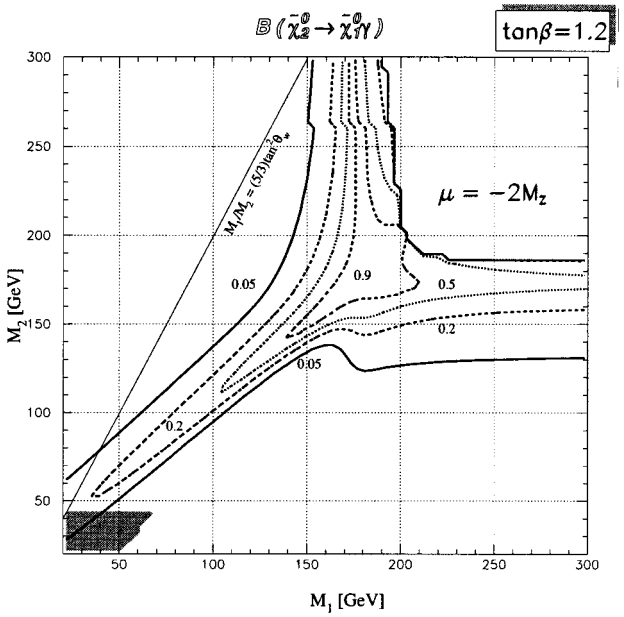

FIG. 9. Contour plot for the neutralino radiative decay BR in the case tanβ=1.2 and $\mu=-2M_Z$. The sfermion masses are all taken degenerate and equal to 1 TeV and m_A=300 GeV. The shaded region is excluded by LEP1–1.5 data.

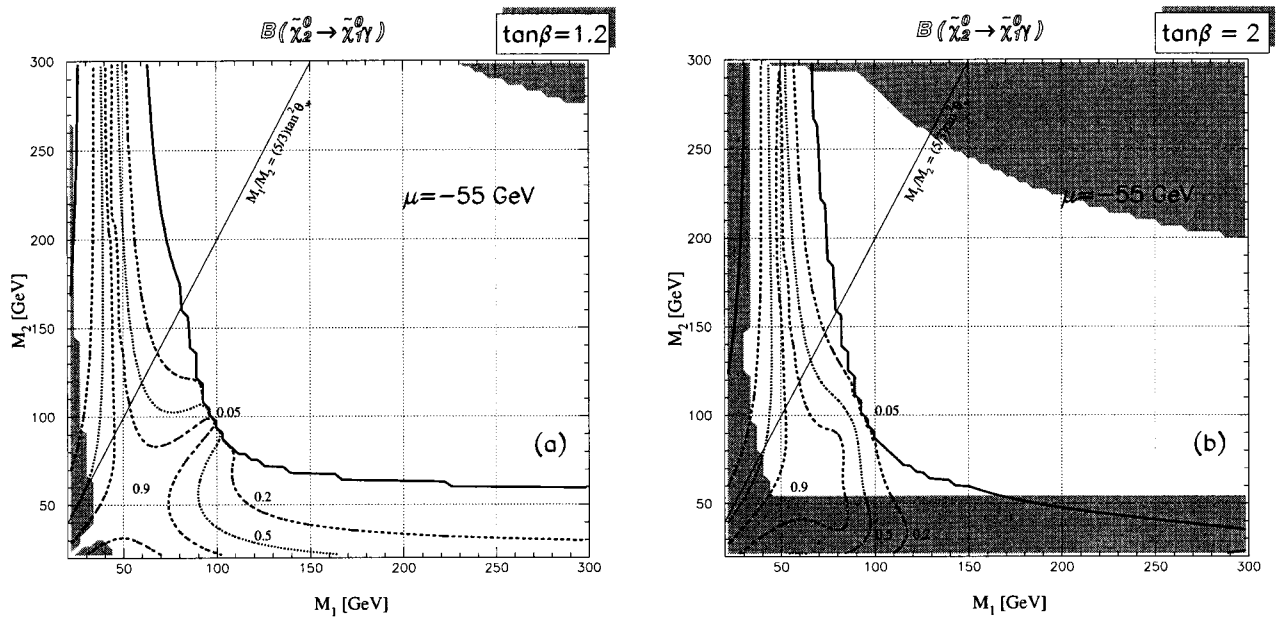

FIG. 10. The same as in Fig. 9, but for $\mu=-55$ GeV and $\tan\beta=1.2$ (a) and 2 (b).

VI. TOP-SQUARK SECTOR INFLUENCE ON $B(\tilde{\chi}_2^0 \to \tilde{\chi}_1^0 \gamma)$

As long as $m_{\tilde{\chi}_1^\pm} \lesssim M_W$, the main contributions to the $\tilde{\chi}_2^0$ radiative decay width come from the $W^\pm/\tilde{\chi}^\mp$ loops (cf. Fig. 1), unless one considers scenarios with light top squarks, i.e., 60 GeV$\lesssim m_{\tilde{t}} \lesssim m_t$ (throughout this paper we assume $m_t=175$ GeV). In the latter case, the amplitudes corresponding to $t/\tilde{t}$ loops are non-negligible and can interfere destructively with the $W^\pm/\tilde{\chi}^\mp$ loops, hence decreasing the radiative decay width. If one assumes the mass of the heavy top-squark $\tilde{t}_2$ sufficiently larger than m_t, then the bulk of this effect comes from the light top-squark $\tilde{t}_1$. Note that the particular values of the other sfermion masses have an important influence just on the tree-level neutralino decay widths, hence affecting only the BR of the radiative decay. The opposite happens for the top-squark parameters, which directly influence the radiative width, and are not involved in the tree-level decays in the parameter ranges considered here. In the previous sections, we assumed the two top-squarks $\tilde{t}_1$ and $\tilde{t}_2$ degenerate, with a mass equal to all the other squark masses. Here, we relax this simplification and consider the effects of assuming different values for $m_{\tilde{t}_1}$ and $m_{\tilde{t}_2}$ and, in particular, the possibility of a rather light $\tilde{t}_1$. In addition, since the mass eigenstates $\tilde{t}_{1,2}$ can be superpositions of the interaction eigenstates $\tilde{t}_{L,R}$, we also take into account the effect of varying the top-squark mixing angle θ_t, defined by $\tilde{t}_1 = \cos\theta_t \tilde{t}_L + \sin\theta_t \tilde{t}_R$; $\tilde{t}_2 = -\sin\theta_t \tilde{t}_L + \cos\theta_t \tilde{t}_R$.

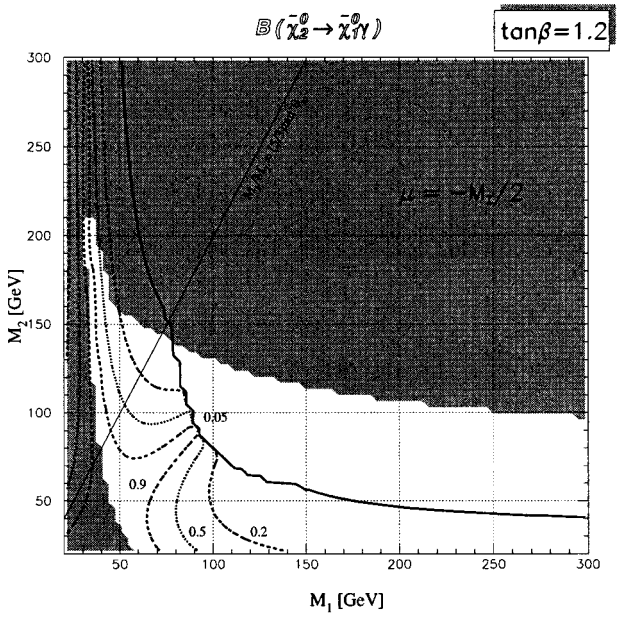

FIG. 11. The same as in Fig. 9, but for $\mu=-M_Z/2$ and $\tan\beta=1.2$.

In Fig. 12, we show the contour plot of $B(\tilde{\chi}_2^0 \to \tilde{\chi}_1^0 \gamma)$ as a function of the two top-squark masses, for four values of the mixing angle θ_t and for two interesting choices of the neutralino sector parameters which correspond to large-$B(\tilde{\chi}_2^0 \to \tilde{\chi}_1^0 \gamma)$ scenarios with different characteristics. Here, we assume degenerate slepton masses of 300 GeV and the other squark masses all equal to 400 GeV. The pseudoscalar Higgs boson mass is fixed at 300 GeV.

Here we did not put any restriction on the $(m_{\tilde{t}_1}, m_{\tilde{t}_2})$ plane (besides a rough direct limit of about 60 GeV on the top-squark masses from LEP data) and we considered the physical masses $m_{\tilde{t}_i}$ as independent parameters. However, in the framework of the MSSM, even without precise unification assumptions in the scalar sector, one usually derives the physical sfermion masses and the L-R mixing angles from the soft SUSY-breaking parameters (i.e., $\tilde{m}_{q_L}$, $\tilde{m}_{u_R}$, $\tilde{m}_{d_R}$, ..., A_t, A_b, ...) as well as from μ and $\tan\beta$ (cf., e.g., Ref. [27]). Once the values of the squark masses of the first two families are fixed to be roughly degenerate, e.g., at 400 GeV as in Fig. 12, and assuming the mass parameters in the sbottom sector to have similar values as well (in particular $\tilde{m}_{b_L} = \tilde{m}_{t_L}$), then it seems unnatural to build a coherent model with the heavy top-squark $\tilde{t}_2$ considerably lighter than 400

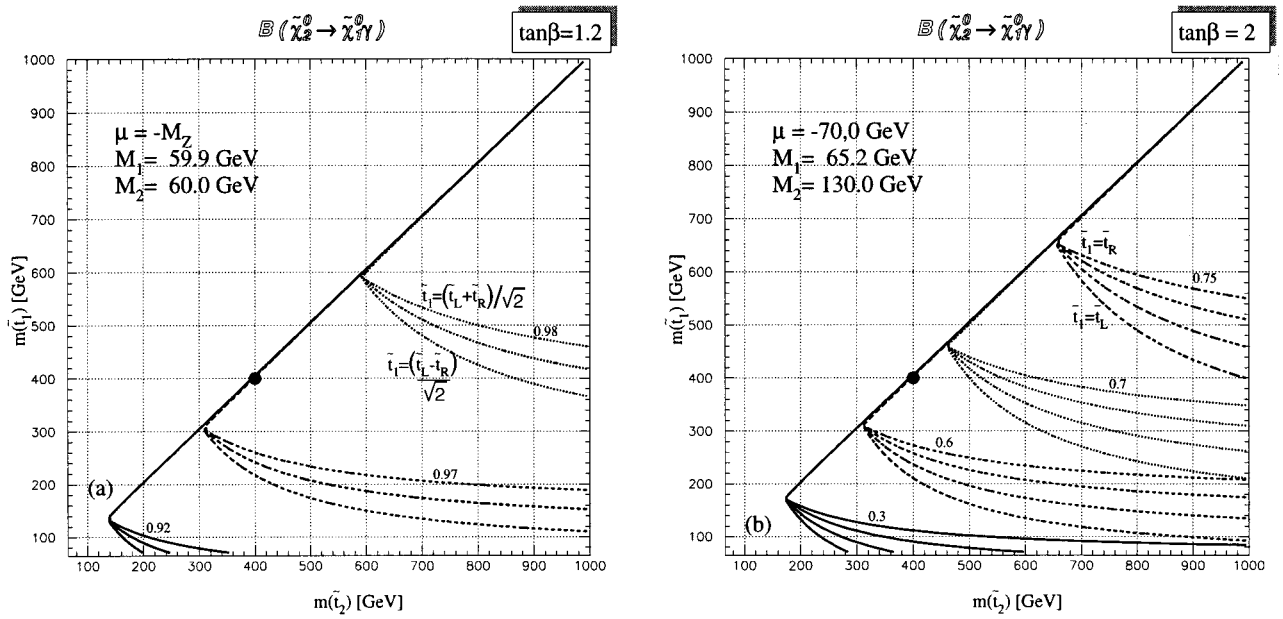

FIG. 12. Contour plot for $B(\tilde{\chi}_2^0 \to \tilde{\chi}_1^0\gamma)$ in the $(m_{\tilde{t}_1}, m_{\tilde{t}_2})$ plane. For each fixed value of $B(\tilde{\chi}_2^0 \to \tilde{\chi}_1^0\gamma)$, four curves corresponding to different choices of the mixing angle θ_t are shown with lines of the same style. Going from the lower curve towards the upper one, one has: (a) Typical dynamical enhancement scenario: $\theta_t = -\pi/4$, 0 (or $\pi/2$), $+\pi/4$; (b) Special kinematical enhancement scenario with gaugino mass unification: $\theta_t = 0$, $-\pi/4$, $+\pi/4$, $+\pi/2$. The other squark masses are taken degenerate and equal to 400 GeV and the slepton masses are set at 300 GeV. Also, $m(A^0) = 300$ GeV. The big black dot corresponds to assuming the top squark masses equal to the other squark masses, as in the previous sections.

GeV, especially when $\tilde{t}_1$ is very light. Similarly, the light top-squark is usually lighter than the other squarks. Furthermore, one has to take into account the influence of the top-squark sector on the light Higgs boson mass m_h through the radiative corrections (cf., e.g., Ref. [27]). Especially for low $\tan\beta$ and for moderate m_A, the presence of a very light $\tilde{t}_1$ ($m_{\tilde{t}_1} \lesssim 70-80$ GeV) may induce m_h to fall below the present experimental limits [i.e., 44 GeV or roughly $\sin^2(\beta-\alpha)\times 60$ GeV, from Ref. [19]], unless $\tilde{t}_2$ is very heavy ($m_{\tilde{t}_2} \gtrsim 1$ TeV). The value $m_A = 300$ GeV we used in this section generally makes the latter problem negligible, but the discussion above still suggests that some regions of the top-squark mass plane we show in Fig. 12 may not correspond to a physically acceptable scenario. Nevertheless, having this in mind, Fig. 12 and the following one provide useful hints to evaluate the pattern of the top-squark sector influence on $B(\tilde{\chi}_2^0 \to \tilde{\chi}_1^0\gamma)$.

In Fig. 12(a), we present a typical case of dynamical enhancement ($M_1 \simeq M_2 = 60$ GeV, $\mu = -M_Z$, and $\tan\beta = 1.2$), while, in Fig. 12(b), a special case of kinematical enhancement is considered. The latter (with $M_1 = 65.2$ GeV, $M_2 = 130$ GeV, $\mu = -70$ GeV, and $\tan\beta = 2$) does not optimize the kinematical mechanism, but has two interesting features. First, the case (b) satisfies the gaugino mass unification relation $M_1 = \frac{5}{3}\tan^2\theta_W M_2$. Second, the value of $\tan\beta$ quite different from 1 gives rise to a sizeable mass splitting between the neutralinos ($\simeq 17$ GeV) and to rather energetic photons, even after the radiative decay of a *soft* $\tilde{\chi}_2^0$. Furthermore, in the case (b) a certain amount of dynamical enhancement is also present.

For each fixed value of the radiative BR, we show how the contours move when varying the mixing angle θ_t. In particular, for a given $B(\tilde{\chi}_2^0 \to \tilde{\chi}_1^0\gamma)$, we present four contours corresponding to $\theta_t = 0$, $-\pi/4$, $\pi/4$, and $\pi/2$. This ordering corresponds to going from the lower curve to the upper one with the same line style in Fig. 12(b), while, in Fig. 12(a), the lower curve is obtained for $\theta_t = -\pi/4$, the upper one for $\theta_t = +\pi/4$, and the curve in the middle corresponds to the almost degenerate contours for $\theta_t = 0$ and $\pi/2$. As a reference, we also show by a big black dot the scenario of complete squark mass degeneracy [in particular $m_{\tilde{t}_{1,2}} = m(\tilde{q}) = 400$ GeV], assumed in the previous analysis. Under that hypothesis, one would obtain $B(\tilde{\chi}_2^0 \to \tilde{\chi}_1^0\gamma) \simeq 97.5\%$ in the case (a) and $B(\tilde{\chi}_2^0 \to \tilde{\chi}_1^0\gamma) \simeq 65\%$ in the case (b). As anticipated, the radiative BR increases with the top squark masses, showing a larger sensitivity to $m_{\tilde{t}_1}$. Indeed, when the mass splitting $(m_{\tilde{t}_2} - m_{\tilde{t}_1})$ is sizable, $B(\tilde{\chi}_2^0 \to \tilde{\chi}_1^0\gamma)$ gets independent of the heaviest mass $m_{\tilde{t}_2}$.

As for the physical composition of the top-squark mass eigenstates entering the radiative decay loops, Fig. 12(b) shows that a lightest top-squark corresponding to a pure $\tilde{t}_R$ ($\theta_t = \pi/2$) is more effective in reducing the radiative BR in the considered case of kinematical enhancement. Indeed, for a fixed $m_{\tilde{t}_1}$, taking $\tilde{t}_1 = \tilde{t}_R$ gives rise to a larger cancellation between the $t/\tilde{t}_1$ and the $W^\pm/\tilde{\chi}^\mp$ loops than in the $\tilde{t}_1 = \tilde{t}_L$ case. The mixed cases corresponding to $\theta_t = \pm\pi/4$ fall in the middle of the two pure cases. In the dynamical enhancement scenario of Fig. 12(a), the behavior is somehow opposite. It turns out that taking a pure $\tilde{t}_L$ or $\tilde{t}_R$ state as the lightest top squark cannot be distinguished in $B(\tilde{\chi}_2^0 \to \tilde{\chi}_1^0\gamma)$, while if $\tilde{t}_1$ is the symmetric (antisymmetric) combination $[\tilde{t}_L + (-)\tilde{t}_R]/\sqrt{2}$, the contributions from the $t/\tilde{t}$ loops are maximized (minimized) and the same happens to the larger destructive interferences with the $W^\pm/\tilde{\chi}^\mp$ loops. This is because in the case (a) the two neutralinos are an almost pure photino and an almost pure $\tilde{H}_b$, which both couple with the

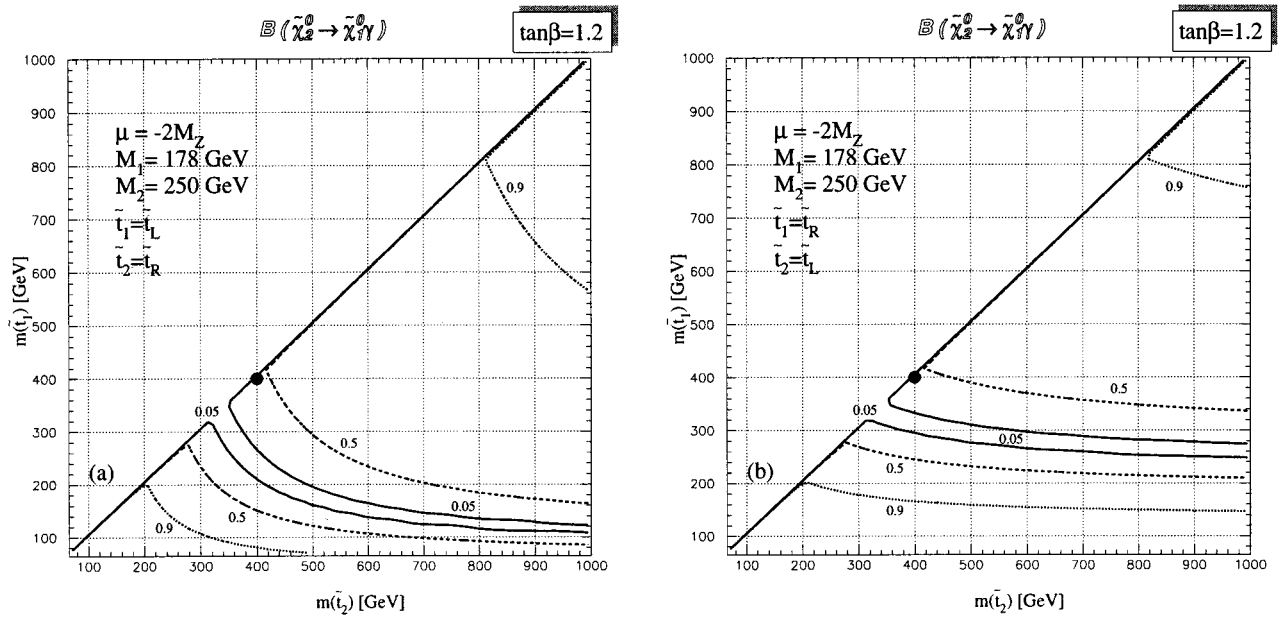

FIG. 13. As in Fig. 12, but for a typical case of kinematical enhancement. In (a) the case $\theta_t=0$, $\tilde{t}_1=\tilde{t}_L$ is shown; in (b) $\theta_t=\pi/2$, $\tilde{t}_1=\tilde{t}_R$.

same strength to left- or right-type standard fermions and sfermions.

As a consequence, the contributions from pure $t/\tilde{t}_L$ and $t/\tilde{t}_R$ loops are almost equal, while, if the mass eigenstate considered is an antisymmetric combination, its contribution to the matrix element is negligible. When this is the case for $\tilde{t}_1$, and $\tilde{t}_2$ is heavy, the whole top squark sector does not contribute and the process is dominated by $W/\chi^{\pm}$ loops.

In the case (b), instead, the $\tilde{\chi}^0_{1,2}$ composition is more involved, with sizable Z-ino components, which distinguish between $f_L\tilde{f}_L$ and $f_R\tilde{f}_R$.

Comparing Fig. 12(a) and 12(b), one notes that varying the top-squark masses can influence the radiative BR more drastically in the case of the kinematical enhancement (b), due to the presence of considerably mixed neutralino states, which increases the relative importance of the amplitudes from $t/\tilde{t}$ loops with respect to the ones from $W^{\pm}/\tilde{\chi}^{\mp}$ loops. For instance, assuming $m_{\tilde{t}_2}\approx 1$ TeV, increasing $m_{\tilde{t}_1}$ from about 100 GeV to about 1 TeV enhances $B(\tilde{\chi}^0_2\to\tilde{\chi}^0_1\gamma)$ by a few percent, in the case (a). On the contrary, in the case (b), the same growth of the lightest top-squark mass gives rise to a wide increase (of order 100%) of the radiative BR.

Such effect is even more dramatic in the case of Fig. 13. Here, a typical scenario with *full* kinematical enhancement is shown, with $M_1=178$ GeV, $M_2=250$ GeV, $\mu=-2M_Z$, and $\tan\beta=1.2$. The corresponding, nearly degenerate, neutralino masses are $m_{\tilde{\chi}^0_1}=180$ GeV and $m_{\tilde{\chi}^0_2}=185$ GeV. Compared to the cases shown in Fig. 12, in the scenario of Fig. 13 the relative weight of the $W^{\pm}/\tilde{\chi}^{\mp}$ and $t/\tilde{t}$ loops in the radiative decay matrix element is rather different. Indeed, the $W^{\pm}/\tilde{\chi}^{\mp}$ and $t/\tilde{t}$ amplitudes depend on $(m_{\tilde{\chi}^{\pm}}/M_W)^2$ and $(m_t/m_t)^2$, respectively (cf. Refs. [16, 6]), and here one has $m_{\tilde{\chi}^{\pm}_1}$ as large as 196 GeV. Thus, the $t/\tilde{t}$ and $W^{\pm}/\tilde{\chi}^{\mp}$ amplitudes turn out to be of the same order of magnitude, with different sign. Then, one expects that for $m_{\tilde{t}_1}\sim 300$ GeV (or possibly more, if the heavier stop is also rather light) the two contributions tend to cancel each other, drastically reducing $B(\tilde{\chi}^0_2\to\tilde{\chi}^0_1\gamma)$ at the level of a few percent. On the other hand, when the top squarks, and in particular $\tilde{t}_1$, are much lighter (heavier) than 300 GeV, the $t/\tilde{t}(W^{\pm}/\tilde{\chi}^{\mp})$ loops dominate, the destructive interferences are negligible, and the $B(\tilde{\chi}^0_2\to\tilde{\chi}^0_1\gamma)$ can comfortably approach the 100% level. This effect is clearly visible in Fig. 13. The influence of a different top-squark mixing can be extracted by comparing Fig. 13(a) and Fig. 13(b), where the *pure* cases $\tilde{t}_1=\tilde{t}_L$ and $\tilde{t}_1=\tilde{t}_R$, respectively, are considered.

VII. CONCLUSIONS

In this paper, we showed that SUSY scenarios where the radiative mode for the next-to-lightest neutralino decay is dominant do exist and can be naturally realized, especially when relaxing the electroweak gaugino mass unification assumptions at the GUT scale. We found that very large $B(\tilde{\chi}^0_2\to\tilde{\chi}^0_1\gamma)$'s are obtained when $\tan\beta\simeq 1$ and/or $M_1\simeq M_2$, with negative μ. When $M_1=(5/3)\tan^2\theta_W M_2$, it is still possible to achieve a large radiative BR, provided $\tan\beta\simeq 1$ and $\mu<0$. Two different mechanisms, which have different phenomenological implications, can be responsible for the radiative BR enhancement. The dynamical mechanism may give rise to signatures including a hard photon and missing energy at hadron colliders, where $\tilde{\chi}^0_2$ can be copiously produced either in association with a $\tilde{\chi}^{\pm}_i/\tilde{\chi}^0_j$ or through the decays of heavier sfermions. On the other hand, at LEP2, in a scenario with $B(\tilde{\chi}^0_2\to\tilde{\chi}^0_1\gamma)$ dynamical enhancement, the main neutralino production channel $e^+e^-\to\tilde{\chi}^0_1\tilde{\chi}^0_2$ (giving rise to a $\gamma+\not{E}$ signature) is quite depleted, requiring either gaugino or Higgsino sizeable components in both $\tilde{\chi}^0_1$ and $\tilde{\chi}^0_2$. At larger c.m. energy e^+e^- colliders [such as the proposed next linear collider (NLC)], the dynamical enhancement of the radiative $\tilde{\chi}^0_2$ decay may be relevant when the $\tilde{\chi}^0_2$ is produced in association with a $\tilde{\chi}^0_j$ with $j>1$, giving rise to signatures containing at least a hard photon and missing energy. On the other hand, the kinematical enhancement (which implies rather degenerate light neutralinos) can give rise to sizable rates for final photons of moderate energy in both hadron and

e^+e^- collisions, provided the next-to-lightest neutralino is produced with energy large enough to boost the rather soft photon.

Finally, an enhanced $\tilde{\chi}_2^0$ decay into a photon might be of relevance for explaining, in the MSSM framework, the $e^+e^-\gamma\gamma+\not{E}_T$ event observed by CDF at the Fermilab Tevatron, that is presently one of the most interesting hints for possible physics beyond the SM.

ACKNOWLEDGMENTS

We would like to thank T. Gherghetta, G. L. Kane, G. D. Kribs, and S. P. Martin for useful discussions and suggestions. S.A. was supported mainly by the I.N.F.N., Italy. S.A. also thanks Professor Gordy Kane and the Particle Theory Group at the University of Michigan for hospitality and additional support.

[1] H. E. Haber and G. L. Kane, Phys. Rep. **117**, 75 (1985).
[2] J. F. Gunion, H. E. Haber *et al.*, Int. J. Mod. Phys. A **4**, 1145 (1987); J. F. Gunion and H. E. Haber, Phys. Rev. D **37**, 2515 (1988).
[3] S. Ambrosanio and B. Mele, Phys. Rev. D **52**, 3900 (1995).
[4] H. Baer, C. H. Chen, C. Kao, and X. Tata, Phys. Rev. D **52**, 1565 (1995).
[5] S. Ambrosanio and B. Mele, Phys. Rev. D **53**, 254 (1996).
[6] H. E. Haber and D. Wyler, Nucl. Phys. **B323**, 267 (1989).
[7] S. Park, *Search for New Phenomena in CDF*, 10th Topical Workshop on Proton-Antiproton Collider Physics, edited by R. Raja and J. Yoh (AIP, New York, 1995).
[8] S. Ambrosanio, G. L. Kane, G. D. Kribs, S. P. Martin, and S. Mrenna, Phys. Rev. Lett. **76**, 3498 (1996).
[9] S. Dimopoulos, M. Dine, S. Raby, and S. Thomas, Phys. Rev. Lett. **76**, 3494 (1996).
[10] S. Ambrosanio, G. L. Kane, G. D. Kribs, S. P. Martin, and S. Mrenna, Phys. Rev. D (to be published).
[11] G. Bhattacharyya and R. N. Mohapatra, Phys. Rev. D **54**, 4204 (1996); J. L. Lopez and D. V. Nanopoulos, Mod. Phys. Lett. A **10,** 2473 (1996); J. Hisano, K. Tobe, and T. Yanagida, Phys. Rev. D **55,** 411 (1997).
[12] For recent examples, see M. Dine and A. E. Nelson, Phys. Rev. D **48**, 1277 (1993); M. Dine, A.E. Nelson, and Y. Shirman, *ibid.* **51**, 1362 (1995), M. Dine, A. E. Nelson, Y. Nir, and Y. Shirman, *ibid.* **53**, 2658 (1996).
[13] P. Fayet, Phys. Lett. **70B**, 461 (1977); **86B**, 272 (1979); **175B**, 471 (1986).
[14] S. Ambrosanio, G. L. Kane, G. D. Kribs, S. P. Martin, and S. Mrenna, Phys. Rev. D **54**, 5395 (1996).
[15] L. E. Ibáñez and G. G. Ross, Phys. Lett. **110B**, 215 (1982); K. Inoue, A. Kakuto, H. Komatsu, and S. Takeshita, Prog. Theor. Phys. **68**, 927 (1982); **71**, 413 (1984); L. Alvarez-Gaumé, M. Claudson, and M. B. Wise, Nucl. Phys. **B207**, 96 (1982); J. Ellis, D. V. Nanopoulos, and K. Tamvakis, Phys. Lett. **121B**, 123 (1983).
[16] H. Komatsu and J. Kubo, Phys. Lett. **157B**, 90 (1985); Nucl. Phys. **B263**, 265 (1986); H. E. Haber, G. L. Kane, and M. Quirós, Phys. Lett. **160B**, 297 (1985); Nucl. Phys. **B273**, 333 (1986); G. Gamberini, Z. Phys. C **30**, 605 (1986).
[17] A. Bartl, H. Fraas, and W. Majerotto, Nucl. Phys. **B278**, 1 (1986).
[18] A. Bartl, H. Fraas, W. Majerotto, and N. Oshimo, Phys. Rev. D **40**, 1594 (1989).
[19] Particle Data Group, L. Montanet *et al.*, Phys. Rev. D **50**, 1173 (1994); 1996 edition available on the PDG WWW pages (URL =http://pdg.lbl.gov).
[20] J. L. Feng, N. Polonsky, and S. Thomas, Phys. Lett. B **370**, 95 (1996).
[21] L3 Collaboration, M. Acciarri *et al.*, Phys. Lett. B **350**, 109 (1995).
[22] G. F. Giudice and A. Pomarol, Phys. Lett. B **372**, 253 (1996).
[23] D. Pierce and A. Papadopoulos, Nucl. Phys. **B430**, 278 (1994).
[24] J. Ellis, J. M. Frere, J. S. Hagelin, G. L. Kane, and S. T. Petcov, Phys. Lett. **132B,** 436 (1983); S. T. Petcov, *ibid.* **139**, 421 (1984); S. M. Bilenky, N. P. Nedelcheva, and S. T. Petcov, Nucl. Phys. **B247**, 61 (1984).
[25] M. M. El Kheishen, A. A. Shafik, and A. A. Aboshoushu, Phys. Rev. D **45**, 4345 (1992); V. Barger, M. S. Berger, and P. Ohmann, *ibid.* **49**, 4908 (1994).
[26] L3 Collaboration, M. Acciarri *et al.*, Phys. Lett. B **377**, 289 (1996); see also OPAL Collaboration, G. Alexander *et al.*, *ibid.* **377**, 181 (1996).
[27] V. Barger, M. S. Berger, and P. Ohmann, Phys. Rev. D **49**, 4908 (1994), and references therein.